# Spectral properties of the large-negative-$U$ Hubbard model

Henk Eskes
*Lorentz Institute for Theoretical Physics, Leiden University, P.O. Box 9506, NL-2300 RA Leiden, The Netherlands*

Andrzej M. Oleś*
*Max-Planck-Institut für Festkörperforschung, Heisenbergstrasse 1, D-70569 Stuttgart, Federal Republic of Germany*
(Received 11 July 1996)

Using the formalism introduced by Harris and Lange [Phys. Rev. **157**, 295 (1967)] explicit expressions for partial sum rules of the individual Hubbard bands in the large-negative-$U$ limit are derived. The one-particle spectrum, optical spectrum, as well as charge- and spin-response functions are considered. The approach gives a transparent description of the main features of these spectra. The main sum rules depend on only two independent nearest-neighbor expectation values which are estimated in the ground state using numerical calculations, exact results, and linear-spin-wave theory. Simple expressions for the intensities of the upper and lower Hubbard bands in the optical conductivity show that this spectrum is extremely sensitive on details of the ground state. The charge-density wave and superconducting phases are clearly distinguishable and even the transition to the broken-symmetry state may have a detectable influence on the conductivity.
[S0163-1829(97)02404-1]

## I. INTRODUCTION

In recent years the negative-$U$ Hubbard model[1] has attracted considerable attention since it is one of the simplest models leading to ($s$-wave) superconductivity. The interest in the Hubbard model has exploded since the discovery of high-$T_c$ superconductivity in the cuprates and bismuthates, raising fundamental questions such as how large the transition temperature might be and what the consequences of the strong correlations in these materials are. For the cuprates the positive-$U$ variant is the most realistic one. On the contrary, negative-$U$ models apply more directly to compounds containing ''negative-$U$'' ions such as Ga, In, Bi, etc., and to the superconducting bismuth oxides without copper.[2] The $BaPb_{1-x}Bi_xO_3$ and $Ba_{1-x}K_xBiO_3$ compounds have many features in common with a negative $U$ Hubbard model.[1,3] They show both charge-density wave (CDW) and singlet superconducting (SS) phases. The parent compound is a diamagnetic insulator, even though it has a half-filled Bi-6$s$ band.[4] Bi is known to prefer the valencies 3+ and 5+ rather than 4+, indicating an effective negative $U$. When increasing the attractive on-site coupling strength $|U|$, the attractive-$U$ model will go from a weak-coupling BCS superconducting regime to a regime with a spin gap of the order of $|U|$ and preexisting pairs, forming a coherent superconducting state with $T_c \propto t^2/|U|$.[5,6] The transition is smooth,[1,7–9] and $T_c$ has a maximum for intermediate $U$.

Optical[10] and one-particle[11] experiments on the cuprate materials, as well as the optical spectra of titanium oxides,[12] show anomalously fast changes of intensity as a function of the hole or electron doping. These experimental findings are well described by the two-dimensional (2D) single-band repulsive Hubbard model with $U$ of the order of the bandwidth[13–16] and are now well understood.[17–19] In this paper we will investigate whether similar weight changes occur in the attractive model.

One attractive feature of the negative-$U$ Hubbard model ($t>0$),

$$H = V + T - \mu N = -|U| \sum_i n_{i\uparrow} n_{i\downarrow} - t \sum_{i,\delta,\sigma} a^\dagger_{i\sigma} a_{i+\delta,\sigma} - \mu \sum_{i\sigma} n_{i\sigma}, \tag{1.1}$$

is the existence of a transformation to positive-$U$ Hamiltonian for bipartite lattices.[1,20] Here $a^\dagger_{i\sigma}$ is the fermion creation operator, $n_{i\sigma} = a^\dagger_{i\sigma} a_{i\sigma}$, and $\mu$ is the chemical potential. An electron-hole transformation for the down spins, combined with a sign change on one of the sublattices,[1] $a^\dagger_{i\downarrow} = \exp(i\vec{\pi}\cdot\vec{R}_i) b_{i\downarrow}$ [$\vec{\pi} = (\pi, \pi, \ldots)$ for a hypercubic lattice], and $a^\dagger_{i\uparrow} = b^\dagger_{i\uparrow}$ leaves the kinetic ($T$) part of the Hamiltonian (1.1) unchanged and changes the sign of $U$. Apart from an unimportant density-dependent constant there are no further terms appearing. The transformation interchanges charge and spin, and the density operator, or the chemical potential term, in the negative-$U$ model, $n_i = \Sigma_\sigma a^\dagger_{i\sigma} a_{i\sigma}$, becomes the magnetization in the positive-$U$ case, $n_i = b^\dagger_{i\uparrow} b_{i\uparrow} - b^\dagger_{i\downarrow} b_{i\downarrow} + 1$. Thus the negative-$U$ model for arbitrary filling and zero magnetization[21] maps on the repulsive Hubbard model at half filling with its magnetization in the $z$ direction $\sim (b^\dagger_{i\uparrow} b_{i\uparrow} - b^\dagger_{i\downarrow} b_{i\downarrow})$ depending on the original filling fraction $n$. Furthermore, for large $|U|$ the attractive model maps on a Heisenberg pseudospin model with finite magnetization. As an important consequence there is a direct relation between phases in the attractive and repulsive cases.[1,22,23] Antiferromagnetic long-range order (LRO) in the Heisenberg case at $n=1$ is related to a CDW or SS for the attractive model, depending whether the order parameter points in the $z$ direction, or lies in the $(x,y)$ plane. Because of the spin-rotational symmetry of the Heisenberg model it immediately follows

 

that the CDW and SS are degenerate at half filling. Adding a small positive nearest-neighbor repulsion to Eq. (1.1) will stabilize the CDW state.

Applying the above transformation to the global spin operators [generators of the SU(2) rotational symmetry] the three ''$\eta$'' generators of a second SU(2) symmetry are found. Acting with $\eta^+=\Sigma_i e^{i\vec{\pi}\cdot\vec{R}_i}c_{i\uparrow}^\dagger c_{i\downarrow}^\dagger$ on an eigenstate of the Hamiltonian new eigenstates are generated with off-diagonal long-range order ($\eta$ pairing).[24] It has been proven recently that the ground state resulting from such a procedure is superconducting in a broad region of parameters of the extended Hubbard model with attractive $U$.[25]

Another interesting consequence of the mapping between positive-$U$ and negative-$U$ concerns the one-particle spectrum. For large attractive interactions the system will contain only doubly occupied and empty sites. When adding an electron one has to study the motion of a singly occupied site in this background. Reversing the role of charge and spin the one-particle spectrum for arbitrary filling is equivalent to the motion of one hole (the added spin) in a spin background (spin up is identified with an empty site, down with a doubly occupied site) where the density determines the average value of $S^z$.[26] Thus it is related to the extensively studied problem of one hole in the $t$-$J$ model. In particular, at half filling the one-particle spectrum in the positive- and negative-$U$ case are identical.

In this paper we will derive expressions for the spectroscopic intensities of the different Hubbard bands in the large-negative-$U$ limit. These sum rules are expressed in terms of ground-state (thermal) expectation values and the sensitivity of the spectra on ground-state properties will be discussed. First the perturbation method, conveniently expressed in terms of Hubbard operators, will be briefly explained. In Sec. III the one-particle spectrum is discussed. Momentum-integrated and momentum-resolved intensities as well as first and second moments of the bands are derived. We will compare the results with a two-pole ansatz for the spectrum. In Secs. IV and V the partial sums for the optical, spin, and charge spectra, respectively, are obtained. The optical spectrum is shown to be very sensitive on the exact ground-state wave function.

## II. LARGE-$U$ PERTURBATION THEORY

In this section we will briefly describe how to derive partial sum rules for the Hubbard subbands separately. A more detailed account can be found in our previous work.[19] The most convenient derivation of the sum rules is found using Hubbard $X$ operators. In short the idea is the following. First large-$|U|$ ($t\ll|U|$) perturbation theory is applied to decouple the various Hubbard sectors. This leads to new effective fermions whose motion conserves the number of doubly occupied sites. Then any operator can be decomposed into parts, each generating a particular number of doubly occupied sites. Intensities (moments) for the individual bands are obtained from these partial operators.

The $X$ operators are defined as follows:

$$a_{i\sigma}^\dagger=X_i^{\sigma 0}+\lambda_\sigma X_i^{2\bar{\sigma}},$$

$$X_i^{\sigma 0}=a_{i\sigma}^\dagger(1-n_{i\bar{\sigma}}),$$

$$X_i^{2\bar{\sigma}}=a_{i\sigma}^\dagger n_{i\bar{\sigma}}, \tag{2.1}$$

and $\lambda_\sigma=\mp 1$ if the spin $\sigma$ is down (up). $X_i^{qA}$ acting to the right turns state $A$ on site $i$ into state $a$. The label 2 denotes a doubly occupied site, 0 an empty site.

A canonical transformation $S$ is now introduced to decouple the Hubbard sectors to a required particular order in $t/U$. This transformation leads to new, effective fermions $c_{i\sigma}^\dagger$ according to

$$a_{i\sigma}^\dagger=e^S c_{i\sigma}^\dagger e^{-S}, \tag{2.2}$$

which, in contrast to the original fermions, conserve the number of doubly occupied sites.[19] For an arbitrary operator $O$ we define the operator $\tilde{O}$ by

$$O\equiv\mathbf{O}(a),\quad \tilde{O}\equiv\mathbf{O}(c), \tag{2.3}$$

i.e., the operator $\tilde{O}$ is obtained from $O$ by replacing the Fermi operators $a_{i\sigma}$ by the transformed operators $c_{i\sigma}$. The transformation $S$ and the Hamiltonian written in terms of the new fermions,

$$H=e^S\tilde{H}e^{-S}=\tilde{H}+[S,\tilde{H}]+\frac{1}{2}[S,[S,\tilde{H}]]+\cdots, \tag{2.4}$$

are determined by the requirement that

$$[H,\tilde{V}]=0. \tag{2.5}$$

Restricting the physical processes to acting between the subspaces of various number of double occupancies, we introduce the operator $O_{nU}$ defined as that part of an original operator $O$ that changes the potential energy $\tilde{V}$ by $nU$. In particular, the kinetic energy of the new fermions consists of three parts. In terms of the Hubbard operators,

$$\tilde{T}=\tilde{T}_0+\tilde{T}_U+\tilde{T}_{-U},$$

$$\tilde{T}_0=-t\sum_{i,\delta,\sigma}(\tilde{X}_{i+\delta}^{2\bar{\sigma}}\tilde{X}_i^{\bar{\sigma}2}+\tilde{X}_{i+\delta}^{\sigma 0}\tilde{X}_i^{0\sigma}),$$

$$\tilde{T}_U=-t\sum_{i,\delta,\sigma}\tilde{X}_{i+\delta}^{2\bar{\sigma}}\tilde{X}_i^{0\sigma},\quad \tilde{T}_{-U}=-t\sum_{i,\delta,\sigma}\tilde{X}_{i+\delta}^{\sigma 0}\tilde{X}_i^{\bar{\sigma}2}, \tag{2.6}$$

where $\vec{\delta}$ is a nearest-neighbor vector. The operators $\tilde{X}$ are defined as in Eq. (2.3).

The transformation (2.4) is now easily obtained.[17,19] To second order,

$$S=(\tilde{T}_U-\tilde{T}_{-U})\frac{1}{U}+[\tilde{T}_U+\tilde{T}_{-U},\tilde{T}_0]\frac{1}{U^2}. \tag{2.7}$$

Of course the first-order term is well known. It leads to the strong-coupling Hamiltonian,[27] or to the simpler $t$-$J$ model. It is important to note that everything up to now is on the operator level, and therefore applies equally well to both the large-negative- and large-positive-$U$ case. The differences occur only when *expectation values* are evaluated. Let us denote the ground-state (or thermal) average by $\langle\ \rangle$, and the action of an operator on the ground state by $\rangle$. Then for the large-negative-$U$ Hubbard model,

$$\tilde{X}_i^{aA}\rangle = 0, \quad \text{when } A=\uparrow \text{ or } A=\downarrow, \tag{2.8}$$

since there are no sites singly occupied by the transformed fermions. Also note that this is much more restrictive than in the positive-$U$ case, where the respective term only vanishes when $A=2$ (for less than half filling).

The full Hamiltonian on the operator level was given in Ref. 19. Restricting the space to only empty and doubly occupied sites (large negative $U$) this simplifies to the following Hamiltonian in second order:

$$H^{(2)} = -\frac{2t^2}{|U|}\sum_{i,\delta} (\tilde{X}_{i+\delta}^{00}\tilde{X}_i^{22} + \tilde{X}_{i+\delta}^{20}\tilde{X}_i^{02}). \tag{2.9}$$

Since there are only two degrees of freedom per site (empty and doubly occupied site) this can be mapped on a Heisenberg spin model. Identifying the doubly occupied site with pseudospin up and the empty site with pseudospin down, the Hamiltonian can be written in terms of spin operators by using the operator identities,

$$\frac{1}{2}(\tilde{X}_{i+\delta}^{00}\tilde{X}_i^{22} + \tilde{X}_{i+\delta}^{22}\tilde{X}_i^{00}) = \frac{1}{4} - S_{i+\delta}^z S_i^z,$$

$$\tilde{X}_{i+\delta}^{20}\tilde{X}_i^{02} = -S_{i+\delta}^+ S_i^-, \tag{2.10}$$

and introducing the superexchange constant $J=4t^2/|U|$, given as in the positive-$U$ case. A minus sign has been introduced, related to the factor $\exp(i\vec{\pi}\cdot\vec{R}_i)$ mentioned in the Introduction. The full Hamiltonian given by the second-order contribution (2.9) and including the chemical potential term is then transformed to

$$H = \frac{J}{2}\sum_{i,\delta}\left(\vec{S}_i\cdot\vec{S}_{i+\delta} - \frac{1}{4}\right) - \mu\sum_i (2S_i^z + 1). \tag{2.11}$$

There is of course a similar route to obtain the same result using the transformation mentioned in the Introduction.[1] First, one maps the negative-$U$ Hubbard model on the large-positive-$U$ model at half filling. Strong-coupling perturbation theory then leads to the Heisenberg model. Equation (2.11) holds for any filling $n=\Sigma_\sigma\langle n_{i\sigma}\rangle$, and the chemical potential $\mu$ plays a role of the external field, $B=2\mu$, which imposes the constraint on the pseudospin magnetization in $z$ direction away from half filling,[1,20]

$$\langle S_i^z\rangle \Leftrightarrow \frac{1}{2}(1-n). \tag{2.12}$$

We note, however, that the total magnetization commutes with the Hamiltonian and hence the last term in Eq. (2.11) has no influence on the dynamics, but only defines the ground state depending on the electron filling. Hence we do not include $\mu$ below, but rather impose the constraint (2.12).

The classical ground state of the pseudospin Hamiltonian (2.11) at half filling ($n=1$) is antiferromagnetic, with the order parameter pointing in an arbitrary direction. This invariance under pseudospin rotations reflects the degeneracy of the CDW and SS states (see Fig. 1) at $n=1$.[1] Away from half filling the classical SS ''spin-flop'' phase has a lower energy than the CDW phase. The constraint given by Eq. (2.12), determining the angle $\phi$ in Fig. 1, can be enforced by adding a magnetic field along the $z$ axis. This acts as a chemical potential. The order parameter in this case has an antiferromagnetic component in the $(x,y)$ plane, and a ferromagnetic component along the direction of the field.

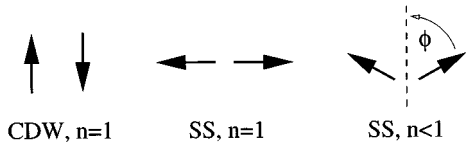


FIG. 1. Schematic representation of the symmetry-broken classical ground state of the pseudospin Hamiltonian (2.11). Pseudospin up (down) represents an empty (doubly occupied) site. The angle $\phi$ between the pseudospin direction and the $z$ axis is a function of the filling, $\cos\phi = 1-n$.

In the following sections we use the above mapping on the pseudospin model (2.11). Since the lowest moments are related to local expectation values, most of the results will depend on the nearest-neighbor spin-spin correlation functions calculated in the ground state of the Heisenberg model with a finite magnetization in the $z$ direction. Because of the symmetry of the problem there are only two independent expectation values,

$$S^{zz} \equiv \langle S_{i+\delta}^z S_i^z\rangle,$$

$$S^{+-} \equiv \langle S_{i+\delta}^+ S_i^-\rangle. \tag{2.13}$$

At half filling $S^{+-}=2S^{zz}$, as long as the symmetry is not spontaneously broken. Note that the total energy is related to $\langle\vec{S}_i\cdot\vec{S}_{i+\delta}\rangle = S^{zz}+S^{+-}$.

The expectation values (2.13) are shown in Fig. 2 as functions of the density $n$ [given by the constraint (2.12)]. The plot shows the results of numerical cluster calculations for the pseudospin Hamiltonian in one and two dimensions up to 20 sites. The nearest-neighbor correlations are only weakly size dependent, and the results should represent the nonbroken symmetry state of an infinite lattice to within a few percent.

In the symmetry-broken state at $n=1$ the relation $S^{+-}=2S^{zz}$ no longer holds, even though the energy per site, related to $S^{+-}+S^{zz}$, will be basically unchanged. We estimate the deviations from the rotationally symmetric state using an extension of linear-spin-wave (LSW) theory. The conventional LSW theory gives a satisfactory estimate of the ground-state energy and the renormalization of the order parameter. However, the errors for the nearest-neighbor spin-spin correlation functions $S^{zz}$ and $S^{+-}$ are large when the lowest-order (LSW) expansion is used. Therefore we have developed an approximate method to estimate these two correlation functions more accurately. This extension of linear-spin-wave theory is described in Appendix A. The numerical results obtained for the 2D and 3D symmetry-broken states are presented in Fig. 2. In the limit of $D\to\infty$ the quantum fluctuations vanish and one finds for the classical SS broken-symmetry state,

$$S^{zz}(D=\infty) = \frac{1}{4}\cos^2\phi = \frac{1}{4}(1-n)^2,$$

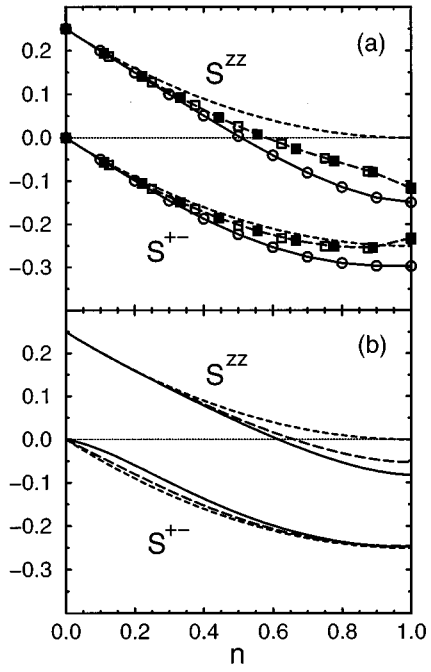


FIG. 2. The nearest-neighbor pseudospin expectation values $S^{zz}$ and $S^{+-}$ as functions of electron density $n$ in the $U<0$ Hubbard model obtained by (a) exact diagonalization of 1D and 2D clusters, and (b) RPA for the 2D (solid lines) and 3D (long-dashed lines) symmetry-broken ground (SS) states. The numerical diagonalization results of the Heisenberg model are given by the open circles, empty squares, and full squares for 20-site ring, 2D 16-site and 18-site clusters, respectively, while full and long-dashed lines in (a) are guides to the eye. The short-dashed lines in (a) and (b) show the expectation values in the classical ground state (at $D\rightarrow\infty$).

$$S^{+-}(D=\infty)=-\frac{1}{4}\sin^2\phi=-\frac{1}{4}n(2-n). \tag{2.14}$$

## III. ONE-PARTICLE SPECTRUM

In this section we consider the momentum-resolved one-particle spectrum, written as the sum of electron addition and removal,

$$A_{\vec{k}\sigma}(\omega)=\sum_f |\langle f,N+1|a^\dagger_{\vec{k}\sigma}|0,N\rangle|^2\delta\{\omega-(E_f^{N+1}-E_0^N)\} + \sum_f |\langle f,N-1|a_{\vec{k}\sigma}|0,N\rangle|^2\delta\{\omega-(E_0^N-E_f^{N-1})\}, \tag{3.1}$$

where $|f,N\pm1\rangle$ denotes a many-particle final state with energy $E_f^{N\pm1}$ and $|0,N\rangle$ is the ground state of the $N$-particle system. The momentum-integrated spectrum is equal to the local spectrum, with $a^{(\dagger)}_{\vec{k}\sigma}$ replaced by $a^{(\dagger)}_{i\sigma}$ in Eqs. (3.1). Note that the electron-removal energies are defined with a minus sign compared to electron addition. With this in mind the labeling of the Hubbard bands below should cause no confusion.

The $l$th moment of the spectrum is

$$m^{(l)}_{\vec{k},\sigma}=\int_{-\infty}^{\infty}d\omega\omega^l A_{\vec{k}\sigma}(\omega) =\langle\{a_{\vec{k}\sigma},[H,\ldots[H,a^\dagger_{\vec{k}\sigma}]], \tag{3.2}$$

where the number of commutators has to be equal to $l$. Since the one-particle basis state $|\vec{k}\rangle$ is either empty or occupied, the total sum rule is simply $m^{(0)}=1$. The photoemission intensity is equal to the occupation number $n_{\vec{k}}$. The first few moments of the total spectrum are easily derived.[28,29]

Below we will calculate moments of the individual Hubbard subbands.[17–19] In order to do so we need to know the potential energy decomposition of $a^\dagger_{i\sigma}$ as shown for the kinetic energy in Eq. (2.6). For the transformed fermions this is simple,

$$c^\dagger_{i\sigma}=c^\dagger_{i\sigma;0}+c^\dagger_{i\sigma;U},\quad c^\dagger_{i\sigma;0}=\tilde{X}^{\sigma 0}_i,\quad c^\dagger_{i\sigma;U}=\lambda_\sigma\tilde{X}^{2\bar{\sigma}}_i. \tag{3.3}$$

The subscript 0 means that the potential energy is unchanged after the particle creation, and $U$ means that the energy is changed by $U$ due to creation of a single doubly occupied site. Therefore $c^\dagger_{i\sigma;0}$ and $c^\dagger_{i\sigma;U}$ describe single-particle excitations into different Hubbard subbands. The above formula demonstrates the usefulness of the $X$-operator formalism. To get a similar expression for the original fermions first one has to apply the transformation Eq. (2.2) and then use the above decomposition. To first order,

$$a^\dagger_{i\sigma;0}=\tilde{X}^{\sigma 0}_i+\frac{t}{U}\sum_\delta(\tilde{X}^{\sigma 0}_{i+\delta}\tilde{X}^{\bar{\sigma}\sigma}_i-\tilde{X}^{\bar{\sigma}0}_{i+\delta}\tilde{X}^{\sigma\bar{\sigma}}_i+\tilde{X}^{\sigma 0}_{i+\delta}\tilde{X}^{22}_i +\tilde{X}^{20}_i\tilde{X}^{\sigma 2}_{i+\delta}), \tag{3.4}$$

and

$$a^\dagger_{i\sigma;U}=\lambda_\sigma\tilde{X}^{2\bar{\sigma}}_i-\lambda_\sigma\frac{t}{U}\sum_\delta(\tilde{X}^{2\bar{\sigma}}_{i+\delta}\tilde{X}^{00}_i+\tilde{X}^{20}_i\tilde{X}^{0\bar{\sigma}}_{i+\delta}+\tilde{X}^{2\bar{\sigma}}_{i+\delta}\tilde{X}^{\sigma\sigma}_i -\tilde{X}^{2\sigma}_{i+\delta}\tilde{X}^{\sigma\bar{\sigma}}_i). \tag{3.5}$$

The operator $a_{i\sigma;-U}=(a^\dagger_{i\sigma;U})^\dagger$ removes a spin from a doubly occupied site, and changes the potential energy of the system by $|U|$. The operator $a^\dagger_{i\sigma;0}$ adds a free spin and leaves the potential energy unchanged. The transitions due to $a^\dagger_{i\sigma;U}$ will then correspond to the lower Hubbard band (LHB), while those due to $a_{i\sigma;0}$ correspond to the upper Hubbard band (UHB).

Equations (3.4) and (3.5) are operator expressions and are valid for both large positive and negative $U$. Below sum rules for the attractive case will be derived. As we will show below, this amounts to taking expectation values with respect to a state with no single occupancies, resulting in a considerable simplification of the final expressions.

### A. Momentum integrated

The weight of the UHB is given by

$$m^{(0)}_0=\langle\{a_{i\sigma;0},a^\dagger_{i\sigma;0}\}\rangle. \tag{3.6}$$

This weight is site and spin independent, taking into account the translational symmetry and using the fact that the spins

are paired; hence the subscript $i\sigma$ is dropped in $m_0^{(0)}$. Adding a spin to a collection of empty and doubly occupied sites will not change the number of doubly occupied sites. Therefore the subscript 0 corresponds to the UHB. On the contrary, removing an electron implies breaking a pair which contributes to the LHB intensity, being $m_{-U}^{(0)}$ with $U<0$. We note that the pair breaking implies an energy increase of order $|U|$ in the final state.

Using Eqs. (3.4), (3.5) and simplifying the resulting expressions for the weights due to the property (2.8) one finds to first order,

$$m_0^{(0)}=\langle \tilde{X}_i^{0\sigma}\tilde{X}_i^{\sigma 0}\rangle=\langle \tilde{X}_i^{00}\rangle=1-\frac{n}{2}+\mathcal{O}(t^2/U^2), \quad (3.7)$$

and

$$m_{-U}^{(0)}=\langle \tilde{X}_i^{22}\rangle=\frac{n}{2}+\mathcal{O}(t^2/U^2). \quad (3.8)$$

The electron-removal (or photoemission) weight has a simple sum rule, being equal to $n/2$. Therefore, to second order, only the LHB is seen in the electron-removal spectrum, and the intensity of the bands simply reflects the number of particles. This is clearly very different from the positive-$U$ case, where the chemical potential moves in one of the bands away from half filling, and a nontrivial redistribution of intensity between the bands follows. In fact, it is easy to prove that to any order in the perturbation series the LHB *is purely electron removal* and the UHB *is purely electron addition*. The fermion operator leaving the band index unchanged, $a_{i\sigma;0}$, is given by a sum of products of the Hubbard operators of the form $\tilde{X}^{aA}\tilde{X}^{bB}\cdots$. The lower- and upper-case letters (referring to the final and initial states, respectively) have to obey two constraints: (i) the number of lower-case 2's has to be equal to the number of upper-case 2's in order to leave the number of doubly occupied sites unchanged, and (ii) the sum of upper-case letters minus the sum of lower-case letters has to be equal to 1 since one electron is removed. Consequently, there is one more $\sigma$ in the sequence $A,B,\ldots$ than in $a,b,\ldots$, and $a_{i,\sigma;0}\rangle=0$. Hence one finds that there is no electron-removal weight in the UHB to any order in perturbation theory. Therefore the chemical potential is always in the gap between the LHB and UHB, for any filling, and to any order in perturbation theory.

Apart from the LHB and UHB, there are higher bands which will have a finite intensity for $t>0$. However, because $[\tilde{T}_{-U},\tilde{X}_i^{\sigma 0}]=0$ and $[\tilde{T}_U,\tilde{X}_i^{2\sigma}]=0$, the operators $a_{i\sigma;-2U}$, etc., are of order $(t/U)^2$, and the intensity of these bands is fourth or even higher order only.[17] This agrees with numerical calculations where hardly any signal of higher bands is observed.

The first moment of the UHB, to order $t$, is given by

$$m_0^{(1)}=\langle\{[c_{i,\sigma;0},\tilde{V}+\tilde{T}_0],c_{i,\sigma;0}^\dagger\}\rangle. \quad (3.9)$$

However, taking the expectation values the term proportional to $t$ vanishes. The energy difference between the UHB and LHB is therefore

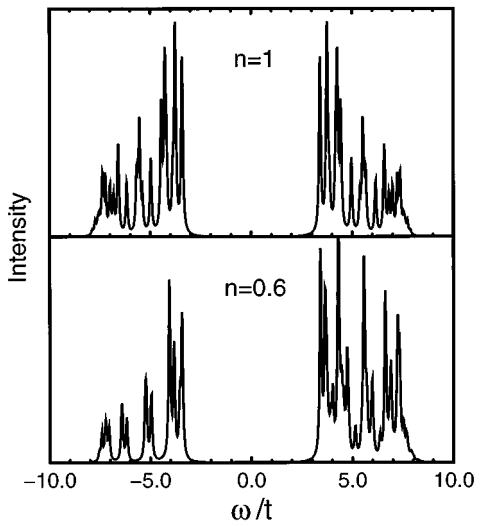


FIG. 3. The momentum-integrated one-particle spectrum for $n=1$ and $n=0.6$ for a chain of ten sites with periodic boundary conditions; $U=-10$, $t=1$. The chemical potential is at $\omega=0$.

$$E^{\mathrm{UHB}}-E^{\mathrm{LHB}}=\frac{m_0^{(1)}}{m_0^{(0)}}-\frac{m_{-U}^{(1)}}{m_{-U}^{(0)}}=|U|+\mathcal{O}(t^2/U). \quad (3.10)$$

There is no energy shift of order $t$. Small corrections of order $t^2/U$ will occur. Compare this with the positive-$U$ case where the separation is larger than $U$ with a correction of order $t$ away from half filling.

In a similar way the width of the Hubbard bands is related to the second moment. For the UHB, to lowest order

$$m_0^{(2)}=\langle\{[c_{i\sigma;0},\tilde{T}_0],[\tilde{T}_0,c_{i\sigma;0}^\dagger]\}\rangle=zt^2\langle\tilde{X}_i^{00}\rangle, \quad (3.11)$$

and

$$(\Delta E^{\mathrm{UHB}})^2\equiv\frac{m_{i\sigma;0}^{(2)}}{m_{i\sigma;0}^{(0)}}-\left(\frac{m_{i\sigma;0}^{(1)}}{m_{i\sigma;0}^{(0)}}\right)^2=zt^2+\mathcal{O}(t^3/U), \quad (3.12)$$

and the same for the LHB. Here $z$ is the number of nearest neighbors. So, to lowest order, the width (second moment) does not depend on the actual occupation $n$ and is equal to the free-particle bandwidth for each band individually. Again, this is different from the repulsive case where the widths depend on the occupation number. Note that the same result can be obtained by using the mapping to the half-filled positive-$U$ case, and Eq. (3.12) is consistent with our previous results.[19] These features of the spectra can be compared with numerical and approximate calculations of the one-particle spectrum.[30–35]

In Fig. 3 we show the numerical spectrum for a ten-site one-dimensional ring. The above derived features of the spectrum are clearly observed. The chemical potential is in the gap. The separation of the bands is close to $|U|$ and the width of both bands is roughly independent of the particle number and is close to the $U=0$ value. The weight of the LHB is simply $n/2$, as given by Eq. (3.8).

### B. Momentum resolved

In contrast to the integrated quantities of the preceding section, the terms proportional to $t$ are no longer zero for the momentum-resolved spectrum. The zeroth moment is calculated using Eq. (3.4) and the definition

$$m^{(0)}_{\vec{k};0}=\frac{1}{N_a}\sum_{i,j} e^{i\vec{k}\cdot(\vec{R}_i-\vec{R}_j)}\langle\{a_{i\sigma;0},a^{\dagger}_{j\sigma;0}\}\rangle, \qquad (3.13)$$

where $N_a$ is the number of sites. Assuming translational invariance for the expectation values and using the one-particle energies,

$$\epsilon_{\vec{k}}=-t\sum_{\delta} e^{i\vec{k}\cdot\vec{\delta}}, \qquad (3.14)$$

one finds, up to order $t/U$,

$$m^{(0)}_{\vec{k};0}=1-\frac{n}{2}+\frac{2\epsilon_{\vec{k}}}{|U|}\langle\tilde{X}^{00}_i\tilde{X}^{22}_{i+\delta}+\tilde{X}^{02}_i\tilde{X}^{20}_{i+\delta}\rangle$$

$$=1-\frac{n}{2}-\frac{2\epsilon_{\vec{k}}}{|U|}\left(\langle\vec{S}_i\cdot\vec{S}_{i+\delta}\rangle-\frac{1}{4}\right), \qquad (3.15)$$

for the momentum-dependent weight of the UHB, and

$$m^{(0)}_{\vec{k};-U}=\frac{n}{2}+\frac{2\epsilon_{\vec{k}}}{|U|}\left(\langle\vec{S}_i\cdot\vec{S}_{i+\delta}\rangle-\frac{1}{4}\right)$$

$$=n_{\vec{k}}+\mathcal{O}(t^2/U^2) \qquad (3.16)$$

for the respective weight of the LHB. Since the weight of the LHB is purely electron removal, $m^{(0)}_{\vec{k};-U}$ is equal to the occupation number $n_{\vec{k}}$. The deviations from $n/2$ increase when $|U|$ decreases, and $n_{\vec{k}}$ is maximal for $\vec{k}$ values close to 0, as expected.

The calculation of the first moment proceeds in a similar way. For the UHB,

$$m^{(1)}_{\vec{k};0}=\epsilon_{\vec{k}}\langle\tilde{X}^{00}_i\tilde{X}^{00}_{i+\delta}-\tilde{X}^{20}_i\tilde{X}^{02}_{i+\delta}\rangle. \qquad (3.17)$$

Dividing by the zeroth moment we obtain the average energies of the bands. One finds for the UHB

$$E_{\vec{k};0}=\epsilon_{\vec{k}}\left[1+\frac{2}{2-n}\left(\langle\vec{S}_i\cdot\vec{S}_{i+\delta}\rangle-\frac{1}{4}\right)\right], \qquad (3.18)$$

and for the LHB

$$E_{\vec{k};-U}=-|U|+\epsilon_{\vec{k}}\left[1+\frac{2}{n}\left(\langle\vec{S}_i\cdot\vec{S}_{i+\delta}\rangle-\frac{1}{4}\right)\right]. \qquad (3.19)$$

The above dispersions depend on the pseudospin order in the ground state, as total spin-spin expectation values enter in both the zeroth and the first moment. Note that these expressions are not symmetric around $n=1$. Nevertheless, the electron-hole symmetry is preserved in the spectra, as the weights of the dispersive part $\sim\epsilon_{\vec{k}}$ are interchanged and the UHB for $n>1$ mirrors the LHB for $n<1$.

At half filling the spectra for positive and negative $U$ are identical, and we have

$$E_{\vec{k};-U}=2\epsilon_{\vec{k}}\left(\langle\vec{S}_i\cdot\vec{S}_{i+\delta}\rangle+\frac{1}{4}\right), \qquad (3.20)$$

as found before in the positive-$U$ case.[19] For Néel order the dispersion vanishes,[36,37] and for (pseudospin) quantum antiferromagnets this average dispersion of the LHB is reversed and narrowed compared to the $U=0$ case.

In Fig. 4 the $\vec{k}$ dependence of the average energy of the LHB is plotted. The numerically obtained weighted average of the pole energies which belong to the LHB for a 1D ten-site ring (the momentum-resolved analog of Fig. 3) is shown and compared with the expressions above. The dispersion *changes sign* roughly around $n=1.25$, and the largest differences between the numerical and perturbative results occur around half filling. At half filling the $k=0$ spectrum lies on average at higher energy than the $k=\pi$ spectrum.

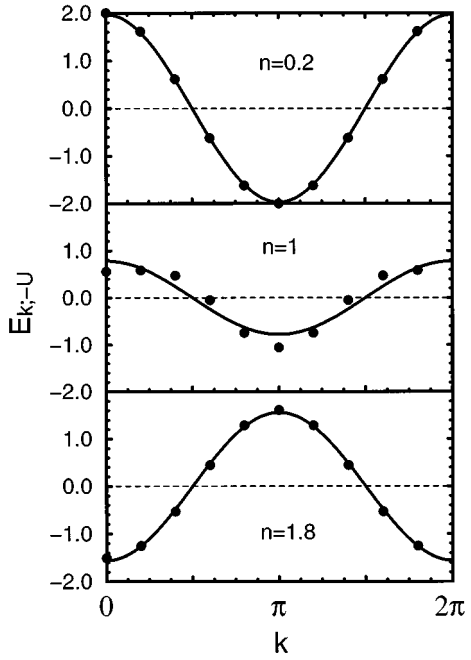


FIG. 4. The momentum-resolved average energy of the LHB in the one-particle spectrum for three different values of the density $n$. Drawn curve is Eq. (3.19) with the expectation values taken from a 20-site Heisenberg ring. Dots are obtained by integrating the LHB part of the momentum-dependent spectrum obtained by exact diagonalization of a ten-site ring with $U=-20$, $t=1$.

The density dependence of the dispersion of the LHB is plotted in Fig. 5, represented by the prefactor $A$ in the energy expression, $E_{\vec{k};-U}=A\epsilon_{\vec{k}}$. The expectation values are obtained from the numerical ground state of a 20-spin Heisenberg ring. Using the Bethe ansatz Griffiths[38] calculated the energy of Heisenberg chain in a magnetic field. His results can be directly used and agree very well with the numerical data. The 2D results are from 16- and 18-site spin clusters.

The limits can be discussed explicitly. One finds in one dimension at half filling $A=1/2-2\ln 2$ from the Bethe solution of the Heisenberg chain. For small $n$, $S^{zz}=1/4-n/2+\mathcal{O}(n^2)$ and $S^{+-}=-n/2+\mathcal{O}(n^2)$. It follows that $E_{\vec{k};-U}=-\epsilon_{\vec{k}}+\mathcal{O}(n)$ and $E_{\vec{k};0}=|U|+\epsilon_{\vec{k}}[1-n+\mathcal{O}(n^2)]$ for small $n$, independent of dimension. The dashed line in Fig. 5, showing the dispersion in the absence of quantum fluctuations, reproduces the limiting behavior for $n\lesssim 2$. Note that the curve suggests that the correction for small $n$ is in fact higher order in $n$, indicating that doubly occupied sites avoid being nearest neighbors.

An approach which is very similar in spirit is the two-pole ansatz for the one-particle spectrum;[28,29] for more references see Ref. 19. Two poles are determined by two energies and two weights. These four parameters are fixed by demanding that they should be consistent with the first four moments of

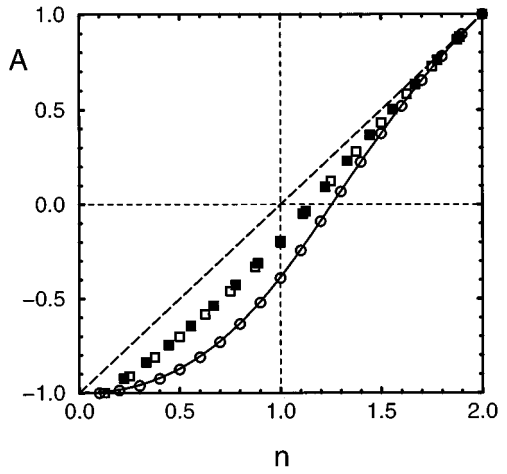


FIG. 5. Prefactor $A$ of the average energy in the LHB ($E_{\vec{k};-U}=A\epsilon_{\vec{k}}$) as a function of electron density $n$. Solid line was obtained using the energy of 1D Heisenberg chain in finite field given in Ref. 38. The numerical results obtained for a 1D 20-site Heisenberg ring, and 16-site (18-site) 2D Heisenberg clusters are shown by circles and empty (filled) squares, respectively. Dashed line indicates the limit of the classical state at $D=\infty$.

the spectral function (the zeroth to third). For large $U$ the poles can be identified as giving the energy averages and weights of the two Hubbard bands. Taking the formulas for the energies and positions from Ref. 29 and expanding to first order we recover precisely the results given by Eqs. (3.15)–(3.19), as shown in Appendix B. We note that the correct coefficient of $\epsilon_{\vec{k}}$ can be obtained only when the complete expression for the third moment is used. In contrast, if the averaging procedure over the Brillouin zone is adopted to calculate the third moment, the results are equivalent to Hubbard I approximation.[34,35]

The two-pole approach has the advantage that it is nonperturbative and gives better results for intermediate values of $U$ (see Ref. 19 for a more extended discussion). On the contrary, the two poles can no longer be identified with Hubbard bands for smaller values of $U$. Already at order $t^2/U$ the two-pole and perturbation method give different results (the poles will acquire some weight from the other band). The two-pole approach clearly cannot be used to study the second and higher moments (width and structure) of the Hubbard subbands, unless one would include the lifetime effects in the model spectral function.

As mentioned in the Introduction, the one-particle spectrum for all fillings $n$ is equivalent to the problem of one hole moving in a spin background.[26] The filling is related to the magnetization by Eq. (2.12). This one-hole problem is well understood in the context of the $t$-$J$ model, and a self-consistent diagrammatic approach (linear-spin-wave ''self-consistent Born'') has been shown to give accurate results. Therefore the spectrum can be discussed in more detail than just the few lowest moments listed above. However, it should be kept in mind that the original fermions are related to the transformed ones by means of Eqs. (3.4) and (3.5), which changes the $\vec{k}$-dependent intensities according to Eq. (3.13). For not too large values of $-U$ this correction to the intensity is considerable. (See, for instance, the plot of $n_k$ in Ref. 19.)

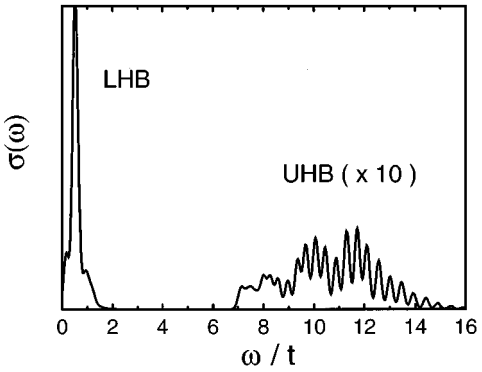


FIG. 6. The optical spectrum at half filling ($n=1$) of a 2D $4\times3$ cluster with open boundary conditions, for $U=-10$ and $t=1$.

More complicated next-nearest-neighbor correlation functions enter into the second moment. The result for the UHB in terms of the $X$ operators is, to order $t^2$,

$$m^{(2)}_{\vec{k};0}=zt^2\frac{2-n}{2}+t^2\frac{1}{N_a}\sum_{i,\delta,\delta',\delta\neq\delta'}e^{i\vec{k}\cdot(\vec{\delta}-\vec{\delta}')}\langle\tilde{X}^{00}_{i+\delta}\tilde{X}^{00}_{i}\tilde{X}^{00}_{i+\delta'}+\tilde{X}^{02}_{i+\delta}\tilde{X}^{22}_{i}\tilde{X}^{20}_{i+\delta'}-2\tilde{X}^{00}_{i+\delta}\tilde{X}^{02}_{i}\tilde{X}^{20}_{i+\delta'}\rangle. \tag{3.21}$$

At half filling this again is equal to the second moment for positive $U$. The explicit result for one dimension and $n=1$ was calculated in our previous paper, Ref. 19. We would like to emphasize that the spectra are mainly incoherent and the width of the momentum-resolved spectra of the two Hubbard bands is on average close to the momentum-integrated one-particle bandwidth at $U=0$, and for $k=\pi/2$ even exceeds this by $\sim$20%. This incoherent width of the spectra is thus very large, a feature completely neglected by the two-pole ansatz. Such an incoherent spectrum results from the bag created by the added free spin which modifies locally the superconducting order parameter.[26]

## IV. OPTICAL SPECTROSCOPY

As in the large-positive-$U$ Hubbard model, the optical conductivity of the negative-$U$ Hubbard model consists of two distinct parts, the LHB and the UHB.[39–41,19] For illustration, we show in Fig. 6 an example of such a spectrum obtained with a 2D $4\times3$ cluster at half filling. The LHB, which corresponds to pair motion, is quite narrow with a width of order $t^2/U$. The UHB has roughly a width $10t$ related to the convoluted kinetic energy of two single electrons. A Hartree-Fock calculation predicts an UHB bandwidth of order $t^2/U$ and therefore underestimates the width of these interband transitions. The current operator is a one-particle operator and therefore necessarily breaks up pairs to lowest order. It is therefore quite remarkable that, in spite of a large value of $U$ which promotes local pairing, the LHB has the largest intensity, while the UHB contains in the present case only $\sim$16% of the total spectral weight. We note that the total weight is underestimated by $\sim$25% due to the open boundary conditions in the cluster, but as we explain below the results of Fig. 6 are representative for the ratio between the weights in the LHB and UHB for a 2D system.

Sum rules for the UHB and LHB features in the frequency-dependent optical conductivity can be derived in a similar way as for the one-particle spectra. The vector potential is coupled to the electrons via the usual Peierls phase factor, changing the Hubbard Hamiltonian (1.1) to

$$H=U\sum_i n_{i\uparrow}n_{i\downarrow}-\sum_{i,\delta,\sigma} t(\vec{\delta})a^{\dagger}_{i\sigma}a_{i+\delta,\sigma}, \tag{4.1}$$

where

$$t(\vec{\delta})=t\exp\left(-\frac{ie}{\hbar c}\vec{A}\cdot\vec{\delta}\right). \tag{4.2}$$

$\vec{A}$ is the vector potential on the bond between $i$ and $i+\delta$. This expression is gauge invariant in the usual way: the effects of a term $\vec{\nabla}f$ added to $\vec{A}$ can be compensated by adding the appropriate phase factor to the wave function.

The expression for the conductivity is obtained from linear response theory.[42–45] The electric field is taken to be homogeneous and pointing in the $x$ direction. Furthermore, we set $\hbar=c=1$. Also the lattice constant $a$ is set to 1. In the Hamiltonian the field couples linearly to the paramagnetic particle current,

$$j_x=it\sum_{i,\delta,\sigma}\delta_x a^{\dagger}_{i+\delta,\sigma}a_{i,\sigma}, \tag{4.3}$$

where as before $\vec{\delta}$ is a vector connecting nearest-neighbor sites. The conductivity per site is related to the current-current correlation function ($\omega\geqslant 0$),

$$\sigma_x(\omega)=D\,\delta(\omega)+\frac{\pi e^2}{\omega N_a}\sum_{f\neq 0}|\langle f,N|j_x|0,N\rangle|^2\,\delta(\omega-E_f+E_0). \tag{4.4}$$

The charge stiffness $D$ (or ''Drude weight'') is given by

$$D=-\frac{2\pi e^2}{zN_a}\langle T\rangle-\frac{2\pi e^2}{\omega N_a}\sum_{f\neq 0}\frac{|\langle f,N|j_x|0,N\rangle|^2}{E_f-E_0}, \tag{4.5}$$

and the total sum rule $W$,

$$W\equiv\frac{1}{\pi e^2}\int_0^{\infty}d\omega\,\sigma_x(\omega)=-\frac{1}{zN_a}\langle T\rangle, \tag{4.6}$$

is proportional to the expectation value of the kinetic energy. Note that only half of the Drude contribution is counted (for $\omega>0$).

In the presence of a vector potential the transformation $S$ is still given by Eq. (2.7) but with the kinetic energy terms changed to

$$\widetilde{T}_U=-\sum_{i,\delta,\sigma} t(\vec{\delta})\widetilde{X}^{2\bar{\sigma}}_{i+\delta}\widetilde{X}^{0\sigma}_i, \tag{4.7}$$

and similarly for $T_{-U}$. The effective Hamiltonian acting within the low energy subspace restricted to doubly occupied and empty sites only is now

$$H=\sum_{i,\delta}\left[\frac{2t^2}{|U|}\left(S^z_iS^z_{i+\delta}-\frac{1}{4}\right)+\frac{2t^2(\vec{\delta})}{|U|}S^+_iS^-_{i+\delta}\right]. \tag{4.8}$$

Only the pseudospin $+-$ part, leading to charge transport, is influenced by the vector potential. Compare this with the large-positive-$U$ case at half filling. The exchange of two real spins does not give rise to charge transport and the Heisenberg Hamiltonian is then found to be field independent.

Since the Hilbert space for large $|U|$ is restricted to empty and doubly occupied sites, and since the ''bare'' kinetic energy breaks up pairs, $\langle\widetilde{T}\rangle=0$ and the kinetic energy expectation value is of order $t^2/U$. Using Eq. (2.6) and the transformation $S$ one finds

$$\begin{aligned}W&=-\frac{1}{zN_a}\langle T\rangle=-\frac{1}{zUN_a}\langle[\widetilde{T}_U-\widetilde{T}_{-U},\widetilde{T}]\rangle+\mathcal{O}(t^3/U^2)\\&=J\left(\frac{1}{4}-\langle\vec{S}_i\cdot\vec{S}_{i+\delta}\rangle\right)+\mathcal{O}(t^3/U^2).\end{aligned} \tag{4.9}$$

The kinetic energy sum rule is equal to the total spin-spin correlation function, including the $z$ part. This is so because also the $S^{zz}$ term originates from virtual excitations of pairs into two spins which delocalizes the spins and therefore decreases the kinetic energy.

The most systematic way to derive the (lowest-order) sum rule for the LHB and UHB consists of expanding the current operator in $x$ direction in an analogous way as the kinetic energy (2.6). To zeroth order,

$$\begin{aligned}j_x&=j_{x;0}+j_{x;U}+j_{x;-U},\\ j_{x;0}&=it\sum_{i,\delta,\sigma}\delta_x(\widetilde{X}^{\sigma 0}_{i+\delta}\widetilde{X}^{0\sigma}_i+\widetilde{X}^{2\bar{\sigma}}_{i+\delta}\widetilde{X}^{\bar{\sigma}2}_i)+\mathcal{O}(t^2/U),\\ j_{x;U}&=it\sum_{i,\delta,\sigma}\delta_x\lambda_{\sigma}\widetilde{X}^{2\bar{\sigma}}_{i+\delta}\widetilde{X}^{0\sigma}_i+\mathcal{O}(t^2/U),\\ j_{x;-U}&=it\sum_{i,\delta,\sigma}\delta_x\lambda_{\sigma}\widetilde{X}^{\sigma 0}_{i+\delta}\widetilde{X}^{\bar{\sigma}2}_i+\mathcal{O}(t^2/U).\end{aligned} \tag{4.10}$$

We consider a finite system with open boundary conditions. The polarization in the $x$ direction, $P_x=\Sigma_{i,\sigma}R_{i,x}n_{i,\sigma}$, is similarly decomposed as follows:

$$\begin{aligned}P_x&=P_{x;0}+P_{x;U}+P_{x;-U},\\ P_{x;0}&=\sum_i R_{i,x}\left(2\widetilde{X}^{22}_i+\sum_{\sigma}\widetilde{X}^{\sigma\sigma}_i\right)+\mathcal{O}(t^2/U^2),\\ P_{x;U}&=\frac{t}{U}\sum_{i,\delta,\sigma}\delta_x\lambda_{\sigma}\widetilde{X}^{2\bar{\sigma}}_{i+\delta}\widetilde{X}^{0\sigma}_i+\mathcal{O}(t^2/U^2),\\ P_{x;-U}&=-\frac{t}{U}\sum_{i,\delta,\sigma}\delta_x\lambda_{\sigma}\widetilde{X}^{\sigma 0}_{i+\delta}\widetilde{X}^{\bar{\sigma}2}_i+\mathcal{O}(t^2/U^2).\end{aligned} \tag{4.11}$$

The paramagnetic current operator is the time derivative of the polarization. Using $j_x=i[H,P_x]$ this is identical to Eq. (4.3). For a finite system with open boundaries the Drude contribution to the conductivity shifts to finite frequency. Replace one of the current operators in Eq. (4.4) by the above commutator. Then the $H$ term cancels the $1/\omega$ term

and the sum rule is easily seen to be equal to $W=i\langle[j_x,P_x]\rangle/(2N_a)=-\langle T_x\rangle/(2N_a)$. The sum rules for LHB and UHB become

$$W_{\mathrm{LHB}}=\frac{i}{2N_a}\langle[j_{x;0},P_{x;0}]\rangle,$$

$$W_{\mathrm{UHB}}=\frac{i}{2N_a}\langle j_{x;U}P_{x;-U}-P_{x;U}j_{x;-U}\rangle. \tag{4.12}$$

These expressions lead to

$$W_{\mathrm{LHB}}=-\frac{4t^2}{U}\frac{1}{N_a}\sum_{i,\delta}(\delta_x)^2\langle\tilde{X}^{20}_{i+\delta}\tilde{X}^{02}_{i}\rangle$$

$$=-2JS^{+-}+\mathcal{O}(t^3/U^2), \tag{4.13}$$

$$W_{\mathrm{UHB}}=\frac{2t^2}{|U|}\frac{1}{N_a}\sum_{i,\delta}(\delta_x)^2\langle\tilde{X}^{22}_{i+\delta}\tilde{X}^{00}_{i}-\tilde{X}^{20}_{i+\delta}\tilde{X}^{02}_{i}\rangle$$

$$=J\left(\frac{1}{4}-S^{zz}+S^{+-}\right)+\mathcal{O}(t^3/U^2). \tag{4.14}$$

Note that, since the intensity is of order $t^2/U$ and since $P_{x;0}$ is of zeroth order, $j_{x;0}$ is needed to first order for the LHB sum rule,

$$j^{(1)}_{x;0}=+\frac{1}{U}[\tilde{T}_U,\tilde{j}_{x;-U}]-\frac{1}{U}[\tilde{T}_{-U},\tilde{j}_{x;U}]. \tag{4.15}$$

Three-site processes[19] do not contribute to $j^{(1)}_{x;0}$ in the subspace of no singly occupied sites and therefore

$$j^{(1)}_{x;0}\rangle=-\frac{4it^2}{U}\sum_{i,\delta}\delta_x\tilde{X}^{20}_{i+\delta}\tilde{X}^{02}_{i}\rangle. \tag{4.16}$$

As could be expected, this describes the motion of pairs instead of single electrons. The above is the current operator in the restricted Hilbert space, and can also be obtained directly from Eq. (4.8). Using now Eq. (4.12) one immediately finds the above result for $W_{\mathrm{LHB}}$ given by Eq. (4.13).

The result for $W_{\mathrm{UHB}}$ (4.14) contradicts the naive expectation that it would dominate as the current breaks up pairs in lowest order. The intensity in UHB is related to the longitudinal pseudospin correlations, or to the nearest-neighbor charge correlation function. It is enhanced by antiferromagnetic pseudospin correlations in $z$ direction, and reduced by the (negative) $S^{+-}$. As given by the above difference, $W_{\mathrm{UHB}}$ is in general quite small in the SS phase, and vanishes in the limit of $D\rightarrow\infty$ for any filling [see Eqs. (2.14)]. In contrast, the intensity in the LHB depends only on $S^{+-}<0$ which measures the kinetic energy of the doubly occupied sites and is thus finite for $0<n<2$. For low densities one finds $W=Jzn/2+\mathcal{O}(n^2)$, and $W_{\mathrm{UHB}}=\mathcal{O}(n^2)$.

At half filling the global spin-rotational symmetry can be combined with the 1D result $\langle\vec{S}_i\vec{S}_{i+1}-1/4\rangle=-\ln 2$. This gives at $n=1$ the total sum rule $W=4t^2\ln 2/|U|$, and the LHB and UHB weight, respectively,

$$W_{\mathrm{LHB}}=\frac{4t^2}{3|U|}(4\ln 2-1)\approx 2.4\frac{t^2}{|U|},$$

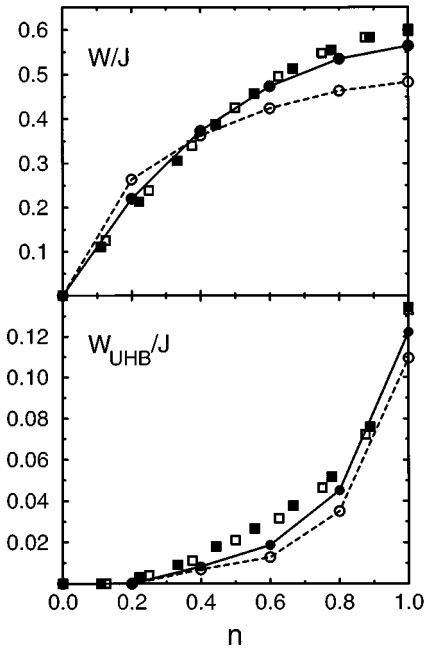


FIG. 7. A comparison of the large-$U$ perturbation results for the total optical sum rule $W/J$ (a), and the intensity of the UHB (b), with integrated intensities obtained for finite $U$ from 2D clusters, as a function of band filling $n$. Numerical results, obtained by integrating the UHB and LHB parts of $\sigma(\omega)$ for a 2D ten-site cluster, are represented by empty and filled circles for $U=-10$ and $U=-20$ ($t=1$). The squares show the sum rules obtained from the Lanczos diagonalization of the 2D Heisenberg clusters of 16 sites (empty squares) and 18 sites (filled squares).

$$W_{\mathrm{UHB}}=\frac{4t^2}{3|U|}(1-\ln 2)\approx 0.4\frac{t^2}{|U|}. \tag{4.17}$$

Unlike in the positive-$U$ Hubbard model,[18,19,40] the weight in the LHB does not vanish at half filling, but represents the *dominating* contribution.

The sum rules derived above are valid in the large-$|U|$ limit. However, the perturbation approach still gives reasonable results for intermediate $U$ of the order of the bandwidth. This is shown in Fig. 7, where the sum rule expressions in two dimensions are compared with numerically integrated $\sigma(\omega)$ spectra of a ten-site Hubbard cluster. For $U=-10$ (the bandwidth is $8t$) the intensities differ from the large-$|U|$ expressions by typically 20%, and the large-$|U|$ approach converges to the numerical sums when $|U|$ increases, as expected. At $n=0.2$, $W_{\mathrm{UHB}}$ is exactly zero. This is a finite-size effect, since the system contains only a single local pair. We have obtained an equally favorable comparison between the numerically integrated sum rules and the large-$|U|$ expressions in one dimension.

The dependence of the spectral weights in the LHB and UHB on the dimensionality is illustrated in Fig. 8. The overall weight in the LHB is largest in one dimension, as the quantum fluctuations are there particularly strong [see Eq. (4.13)]. The observations made above for one dimension concerning the relative intensities [see Eqs. (4.17)] turn out to be quite general—because of the coherent propagation of local pairs there is very little weight in the UHB, and only near half filling does the weight increase significantly. For

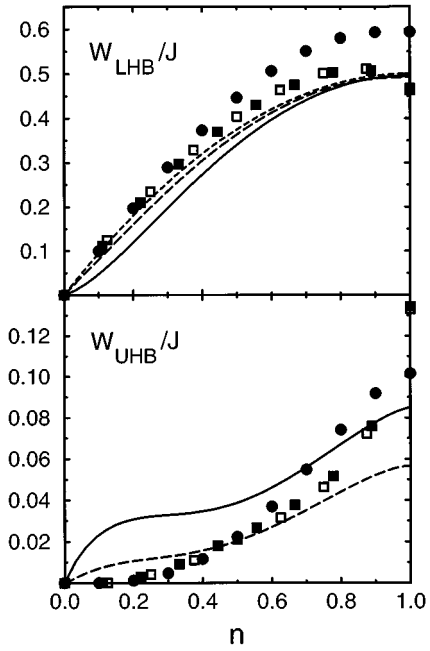


FIG. 8. The optical conductivity sum rules for the LHB, $W_{\mathrm{LHB}}/J$ (a), and for the UHB $W_{\mathrm{UHB}}/J$ (b), as functions of band filling $n$ for $D=1$, 2, 3, and for the classical state at $D=\infty$. The spectral weights are obtained from the spin-spin correlation functions $S^{zz}$ and $S^{+-}$ of the Heisenberg model at finite field. The results obtained for the rotationally invariant states (filled circles for the 1D 20-site ring, empty and filled squares for the 2D clusters of 16 and 18 sites, respectively) are compared with the symmetry-broken SS state in two (solid lines), three (long-dashed lines), and infinite dimensions [dashed line in (a)].

instance, in two dimensions one finds at half filling $W_{\mathrm{UHB}}/W \simeq 23\%$ (see Fig. 7). The increase of the total weight $W$, Eq. (4.9), reflects the increase of the kinetic energy with increasing filling. The data points obtained with 2D clusters show a maximum of $W_{\mathrm{LHB}}$ at $n \simeq 0.87$ (Fig. 8). Unlike in one dimension, this reflects the precursor effect of the symmetry breaking, as $|S^{+-}|>2|S^{zz}|$ for the 2D clusters, except at half filling where $|S^{+-}|=2|S^{zz}|$ due to the rotational symmetry of the ground state in the pseudospin space. The weights found for the LHB in the symmetry-broken SS ground states in two and three dimensions are very similar and approach the analytic result $W_{\mathrm{LHB}}=n(2-n)/2$ in the limit $D\rightarrow\infty$. The symmetry breaking increases the value of the transverse component $S^{+-}$ which has a large contribution from the order parameter in the SS phase (see Fig. 1), and therefore the weight in the UHB is reduced. This trend is reproduced correctly by our random-phase approximation (RPA) calculation close to half filling, but for small $n$ the difference between $S^{+-}$ and $S^{zz}$ in the RPA approach turns out to be not accurate enough, and $W_{\mathrm{UHB}}$ is overestimated. The weight of the UHB vanishes for the classical state in the $D\rightarrow\infty$ limit. This provides the sum rule for the dynamical mean-field theory[46] for the attractive Hubbard model.

The strong sensitivity of the intensities on the ground state of the system is well demonstrated by the data for the rotationally invariant and symmetry-broken states at $n=1$ collected in Table I. In the extreme quantum limit, given by the singlet ground state of a two-site cluster, only the LHB contributes to the conductivity which has the maximal total weight. In contrast, a triplet state (not shown) would give zero total weight and a negative weight in the LHB. The negative weight occurs because the triplet is an excited state and therefore the LHB conductivity is dominated by *emission* instead of absorption. Going from the singlet through a 1D to a 2D system, the weight in the UHB increases gradually, but the total weight goes down. In one dimension the correlation functions $S^{zz}-1/4$ and $S^{+-}$ almost cancel each other, while in two dimensions the quantum fluctuations are less strong and the UHB intensity is larger. The symmetry-broken superconducting (SS) states have their order parameter in the $(x,y)$ planes, which gives again a fast decrease of the UHB weight with increasing dimension, and at $D=\infty$ only the LHB with half of the singlet weight is left. Thus only the coherent motion of the pairs contributes to the conductivity in this limit. The opposite limit is found for the CDW state, where the spins point along the $z$ direction. Here the conductivity is dominated by pair breaking. Note that the RPA-CDW state in 2D still has most of the intensity in the LHB due to the sizable admixture of spin fluctuations. To summarize, by canting the spins from the $(x,y)$ plane (SS phase) to the $z$ direction (CDW phase) *the intensity gets transferred from the LHB to the UHB*.

TABLE I. Spin correlation functions $S^{zz}$ and $S^{+-}$ and optical intensities of the LHB ($W_{\mathrm{LHB}}/J$) and UHB ($W_{\mathrm{UHB}}/J$) for different ground states and dimensions at $n=1$. The two-site singlet state is represented by $D=0$, $S=0$. Rotationally invariant (RI) states in $D=1$ and $D=2$ were obtained by Lanczos diagonalization of the Heisenberg model for a 20-site ring and 18-site 2D cluster, respectively. The symmetry-broken singlet superconducting (SS) and charge-density wave (CDW) states, all below the line, are calculated in RPA for $D=2$ and $D=3$ and compared with the classical states at $D=\infty$.

| $D$ | State | $S^{zz}$ | $S^{+-}$ | $W_{\mathrm{LHB}}/J$ | $W_{\mathrm{UHB}}/J$ |
|---|---|---|---|---|---|
| 0 | $S=0$ | −0.25 | −0.50 | 1.0 | 0.0 |
| 1 | RI | −0.1484 | −0.2968 | 0.5936 | 0.1016 |
| 2 | RI | −0.1157 | −0.2313 | 0.4626 | 0.1344 |
| 2 | SS | −0.0820 | −0.2470 | 0.4940 | 0.0850 |
| | CDW | −0.1650 | −0.1639 | 0.3278 | 0.2511 |
| 3 | SS | −0.0526 | −0.2460 | 0.4920 | 0.0566 |
| | CDW | −0.1935 | −0.1051 | 0.2102 | 0.3384 |
| ∞ | SS | 0.0 | −0.25 | 0.5 | 0.0 |
| | CDW | −0.25 | 0.0 | 0.0 | 0.5 |

## V. CHARGE AND SPIN EXCITATIONS

The dynamical, momentum-dependent charge structure factor is defined as

$$C(\vec{q},\omega)=\sum_f |\langle f,N|n_{\vec{q}}|0,N\rangle|^2\,\delta(\omega-E_f^N+E_0^N), \quad (5.1)$$

with

$$n_{\vec{q}}=\frac{1}{\sqrt{N_a}}\sum_i e^{i\vec{q}\cdot\vec{R}_i}n_i, \quad (5.2)$$

and the sum rule is simply

$$\int_{-\infty}^{\infty} d\omega C(\vec{q},\omega)=\langle n_{-\vec{q}} n_{\vec{q}}\rangle. \tag{5.3}$$

For the partial sums we need the transformed $X_i^{\alpha\beta}$ operators. One finds to first order the number operator for singly occupied sites,

$$X_i^{\sigma\sigma}=\tilde{X}_i^{\sigma\sigma}-\frac{t}{U}\lambda_\sigma\sum_\delta (\tilde{X}_{i+\delta}^{2\bar{\sigma}}\tilde{X}_i^{0\sigma}-\tilde{X}_i^{2\sigma}\tilde{X}_{i+\delta}^{0\bar{\sigma}}-\tilde{X}_{i+\delta}^{\sigma 0}\tilde{X}_i^{\sigma 2}+\tilde{X}_i^{\sigma 0}\tilde{X}_{i+\delta}^{\bar{\sigma}2}), \tag{5.4}$$

and for doubly occupied sites,

$$X_i^{22}=\tilde{X}_i^{22}+\frac{t}{U}\sum_{\delta,\sigma}\lambda_\sigma(\tilde{X}_i^{2\bar{\sigma}}\tilde{X}_{i+\delta}^{0\sigma}+\tilde{X}_{i+\delta}^{\sigma 0}\tilde{X}_i^{\bar{\sigma}2}). \tag{5.5}$$

Using the charge conservation constraint, $n_i=2X_i^{22}+\Sigma_\sigma X_i^{\sigma\sigma}$ and the above expressions, the derivation is straightforward. The intensity is mainly in the LHB,

$$\int_{-\infty}^{\infty} d\omega C^{\mathrm{LHB}}(\vec{q},\omega)=\frac{4}{N_a}\sum_{i,j} e^{i\vec{q}\cdot(\vec{R}_j-\vec{R}_j)}\langle\tilde{X}_i^{22}\tilde{X}_j^{22}\rangle + \mathcal{O}(t^2/U^2). \tag{5.6}$$

This is simply the response function for bosons on a lattice. The charge 2 is reflected by the prefactor 4 in Eq. (5.6). The UHB intensity is second order in $t/U$,

$$\int_{-\infty}^{\infty} d\omega C^{\mathrm{UHB}}(\vec{q},\omega)=\frac{4t^2}{N_a U^2}\sum_{i,\delta}[1-\cos(\vec{q}\cdot\vec{\delta})]\langle\tilde{X}_{i+\delta}^{22}\tilde{X}_i^{00}-\tilde{X}_{i+\delta}^{20}\tilde{X}_i^{02}\rangle$$

$$=\frac{4t^2}{U^2}\left(\frac{1}{4}-S^{zz}+S^{+-}\right)\sum_\delta[1-\cos(\vec{q}\cdot\vec{\delta})]+\mathcal{O}(t^3/U^3). \tag{5.7}$$

The response vanishes at $\vec{q}=0$ and is maximal at $\vec{q}=\vec{\pi}$. For a homogeneous system the expectation value can be taken outside the sum and the $\vec{q}$ dependence is just a simple cosine function. The density dependence is the same as for the UHB in the optical conductivity (see Fig. 7). Because the UHB intensity is second order and because of the small density-dependent prefactor, the UHB will be barely visible in the 3D SS state.[32] As in the optical case the UHB will be more intense in the CDW phase.

The longitudinal spin dynamical structure factor is

$$S_\parallel(\vec{q},\omega)=\sum_f |\langle f,N|S_{\vec{q}}^z|0,N\rangle|^2\delta(\omega-E_f^N+E_0^N), \tag{5.8}$$

where

$$S_{\vec{q}}^z=\frac{1}{\sqrt{N_a}}\sum_i e^{i\vec{q}\cdot\vec{R}_i}\frac{1}{2}(X_i^{\uparrow\uparrow}-X_i^{\downarrow\downarrow}). \tag{5.9}$$

The intensity of the LHB is determined by the expressions of the form $S_{i;0}^z\rangle$, i.e., on the left and on the right there is a state with no singly occupied sites. The intermediate states in second and higher order, obtained by acting with $\tilde{T}_{-U}$, contain singly occupied sites. However, since up and down spins occur in a completely symmetric manner, each up spin contribution is canceled by an identical down spin contribution. Therefore one finds that $S_{i;0}^z\rangle=0$, and

$$\int_{-\infty}^{\infty} d\omega S_\parallel^{\mathrm{LHB}}(\vec{q},\omega)=0, \tag{5.10}$$

to any order in $t/U$. This result proves the existence of a spin gap in the large-negative-$U$ Hubbard model[47]—making a spin excitation implies breaking up pairs and changing the energy by $|U|$.

The operator in Eq. (5.4) does not break up pairs to lowest order and therefore the weight of the UHB is of second order,

$$\int_{-\infty}^{\infty} d\omega S_\parallel^{\mathrm{UHB}}(\vec{q},\omega)=\frac{t^2}{N_a U^2}\sum_{i,\delta}[1-\cos(\vec{q}\cdot\vec{\delta})]\langle\tilde{X}_{i+\delta}^{22}\tilde{X}_i^{00}+\tilde{X}_{i+\delta}^{20}\tilde{X}_i^{02}\rangle=\frac{t^2}{U^2}\left(\frac{1}{4}-\langle\vec{S}_i\cdot\vec{S}_{i+\delta}\rangle\right)\sum_\delta[1-\cos(\vec{q}\cdot\vec{\delta})]+\mathcal{O}(t^3/U^3). \tag{5.11}$$

Again the expectation value factorizes into a $\vec{q}$-dependent and a density-dependent part. The density dependence is given by the full spin-spin correlation function (see Fig. 2) and the $\vec{q}$ dependence is the same as for the charge response.[32]

Finally, we consider the transverse spin structure factor,

$$S_{\perp}(\vec{q},\omega)=\sum_{f}\ |\langle f,N|S_{\vec{q}}^{+}|0,N\rangle|^{2}\delta(\omega-E_{f}^{N}+E_{0}^{N}), \tag{5.12}$$

where

$$S_{\vec{q}}^{+}=\frac{1}{\sqrt{N_a}}\sum_{i}\ e^{i\vec{q}\cdot\vec{R}_i}X_i^{\uparrow\downarrow}. \tag{5.13}$$

The calculation involves the transformed spin-flip operator,

$$X_i^{\sigma\bar{\sigma}}=\tilde{X}_i^{\sigma\bar{\sigma}}-\frac{t}{U}\lambda_{\sigma}\sum_{\delta}\ (\tilde{X}_{i+\delta}^{2\bar{\sigma}}\tilde{X}_i^{0\bar{\sigma}}+\tilde{X}_{i+\delta}^{0\bar{\sigma}}\tilde{X}_i^{2\bar{\sigma}}-\tilde{X}_{i+\delta}^{\sigma 0}\tilde{X}_i^{\sigma 2}-\tilde{X}_{i+\delta}^{\sigma 2}\tilde{X}_i^{\sigma 0}). \tag{5.14}$$

Since $X_i^{\uparrow\downarrow}$ turns a down spin into an up spin, this operator breaks at least one pair to any order in perturbation theory. Thus there is again no spectral weight in the LHB to any order in $t/U$,

$$\int_{-\infty}^{\infty}d\omega S_{\perp}^{\mathrm{LHB}}(\vec{q},\omega)=0. \tag{5.15}$$

The weight of the UHB is of second order, and we simply find that

$$\int_{-\infty}^{\infty}d\omega S_{\perp}^{\mathrm{UHB}}(\vec{q},\omega)=2\int_{-\infty}^{\infty}d\omega S_{\parallel}^{\mathrm{UHB}}(\vec{q},\omega). \tag{5.16}$$

This reflects the rotational symmetry of the (real) spin response, as the ground state is nonmagnetic. Note, however, that the *pseudospin* averages $S^{zz}$ and $S^{+-}$ are highly anisotropic away from half filling, as we have shown in Fig. 2 (or even at half filling due to symmetry breaking).

## VI. SUMMARY AND DISCUSSION

In conclusion we have derived sum rules for the UHB and LHB of the Hubbard model in the limit of large attractive interactions. In this limit only two degrees of freedom per site are left, namely, each site can be either doubly occupied or empty, and the low energy behavior is determined by a (pseudospin) Heisenberg Hamiltonian. The sum rules follow from local correlations (at short time scales) and are written in terms of only two independent correlation functions: the nearest-neighbor $S^{zz}$ and $S^{+-}$ spin-spin correlations (2.13).

The momentum-integrated one-particle spectrum is insensitive to ground-state correlations. The intensity of the LHB (UHB) is given simply by the number of electrons (holes) in the system. The chemical potential is in the gap, the energy separation between the bands is $|U|$, and the width of each of the bands (second moment) is equal to the $U=0$ width. The momentum-resolved energy average, however, is determined by the nearest-neighbor spin correlation function. For $n=0$ the first moment of the UHB is equal to $\epsilon_{\vec{k}}$ (free-particle dispersion) and its momentum dependence decreases with increasing filling. At some $n<1$ this average dispersion *changes sign* and goes to $-\epsilon_{\vec{k}}$ for $n=2$. We have shown that this behavior is correctly reproduced by the two-pole ansatz.

The negative-$U$ Hubbard model has a spin gap and therefore the LHB is missing in the frequency-dependent spin structure factor (5.10). The UHB response is second order in $t/U$, and the density and frequency dependence of the weight factorize. The frequency dependence is a simple cosine function and it vanishes at $\vec{q}=\vec{0}$. The density dependence is given by the total spin-spin correlation function and the weight is proportional to the energy gain due to quantum fluctuations in the Heisenberg system. The charge response is almost purely within the LHB. The UHB occurs in second order, but with only a small prefactor in the superconducting state.

The most spectacular changes as function of electron filling and system dimension were found in the optical spectrum. *The relative weights of the UHB and LHB in $\sigma(\omega)$ depend very sensitively on the actual initial state*—see Table I. Even though these intensities depend on *local* expectation values, subtle effects such as a broken symmetry may have a noticeable effect on the spectra. The LHB intensity is related to the dynamics of double occupancies expressed by the pseudospin fluctuations $\langle S_i^{+}S_{i+\delta}^{-}\rangle$ in the effective Hamiltonian (2.11). It is quite remarkable that the LHB has most of the intensity, both for the rotationally invariant and for the SS state, since the current is a one-particle operator and therefore might be expected to act mainly as a pair breaker. This demonstrates the substantial gain in kinetic energy due to the quantum coherence of the local pairs which represents in this case the leading contribution to the optical conductivity. On the contrary, a CDW state gives an intense UHB and a much reduced but still sizable contribution due to local pairs. The latter results from quantum fluctuations and vanishes completely in the classical limit of the CDW state (at $D\rightarrow\infty$). This shows that the optical spectra of the attractive Hubbard model in two or three dimensions are qualitatively different from the $D\rightarrow\infty$ limit, as calculated by the dynamical mean-field theory.[46] We hope that future calculations will provide more information about the frequency dependence of the optical conductivity in this limit.

It is interesting to compare the optical conductivity in large-$|U|$ limit with the RPA results of Taraphder *et al.*, who found a much stronger weight in the UHB than that of the LHB.[3] However, the ratio of the UHB to the LHB is overestimated by a factor close to 6. We have verified that the calculation of the spectral weight in the LHB based on the split-band picture in the CDW state underestimates the pair contribution to the optical conductivity. This follows from the applied mean-field treatment neglecting the quantum fluctuations of pseudospins, while in this state the latter determine the weight in the LHB due to the spin-spin correlation function $S^{+-}$. Therefore the large-$U$ limit value of $W_{\mathrm{LHB}}$ (4.13) is not reproduced quantitatively using Eq. (F11) of Ref. 3.

It is tempting to compare the results obtained above with experiments on $Ba_{1-x}K_xBiO_3$ and $BaPb_{1-x}Bi_xO_3$. These compounds show a phase diagram which is very similar to the negative-$U$ Hubbard model with an extra nearest-neighbor Coulomb repulsion added. Around half filling

($BaBiO_3$) the materials are diamagnetic and insulating, while after roughly 30% doping they become superconducting. In $BaBiO_3$ there is a gap of about 2 eV which suggests that Coulomb interactions are quite large. In the optical conductivity one observes a strong rearrangement of weight from high to low energy when increasing the doping.[48] Comparing with our sum rules this signals a transition from the CDW to SS phase. Although a quantitative comparison is not possible due to ambiguous experimental resolution of the LHB and UHB features in the optical conductivity, we find it very encouraging that the UHB gradually vanishes under doping in $Ba_{1-x}K_xBiO_3$.[48] However, these changes are accompanied by strong shifts in peak energies, while in the large-$U$ Hubbard model the UHB would stay at a roughly constant energy $U$. Moreover, in undoped $BaBiO_3$ no LHB signal is observed in the conductivity. In Table I we show that even for the CDW in 3D one still expects a considerable LHB signal. We tentatively interpret this difference as originating either from polaronic trapping, or from the reduction of effective $|U|$ by doping. Another possibility is that a nearest-neighbor repulsion suppresses the quantum fluctuations.

We believe that more information about electronic interactions in Bi compounds is needed for making a more quantitative analysis of the experimental data. It is straightforward to include a nearest-neighbor interaction $V$ in the Hamiltonian. Even a small repulsive interaction will stabilize the CDW state near half filling, and lead to a phase diagram which is very similar to that of doped $BaBiO_3$ compounds.[1] However, the coupling to the lattice, which occurs in the CDW state,[49] is expected to modify the kinetic energy and influence the spectral weights in the optical spectroscopy. Thus a purely electronic model might not suffice to reproduce the spectra of these compounds.

## ACKNOWLEDGMENTS

We thank Lou-Fe' Feiner, Peter Horsch, Ginyiat Khalliulin, Roman Micnas, and Jan Zaanen for stimulating discussions. H.E. is supported by the Stichting voor Fundamenteel Onderzoek der Materie (FOM), which is financially supported by the Nederlandse Organisatie voor Wetenschappelijk Onderzoek (NWO). A.M.O. acknowledges the partial support by the Committee of Scientific Research (KBN) of Poland, Project No. 2 P03B 144 08.

## APPENDIX A: LINEAR-SPIN-WAVE THEORY FOR THE SPIN-FLOP PHASE

The classical ground state of the pseudospin model (2.11) is given by a two-sublattice (labeled $A$ and $B$) spin-flop phase (see Fig. 1). The relative angle $2\phi$ between the spins on the two sublattices is directly related to the constraint Eq. (2.12). This constraint can be enforced by introducing an external magnetic field $B_z$ acting in the $z$ direction (2.12). On the mean-field level

$$B_z = 2zJS\cos\phi. \tag{A1}$$

The linear-spin-wave calculation of the elementary excitations may be conveniently performed by using a canonical transformation which leaves the spins in $A$ sublattice unchanged, while it rotates the spin components on the $B$ sublattice ($j \in B$),

$$S_j^z = \overline{S_j^z}\cos(2\phi) + \overline{S_j^x}\sin(2\phi),$$
$$S_j^x = -\overline{S_j^z}\sin(2\phi) + \overline{S_j^x}\cos(2\phi). \tag{A2}$$

As a result, one finds the following transformed Hamiltonian:

$$H = J\sum_{\langle ij\rangle} [\cos(2\phi)\overline{S_i^z S_j^z} + \sin(2\phi)(\overline{S_i^z S_j^x} - \overline{S_i^x S_j^z}) + \tfrac{1}{2}\cos^2\phi(\overline{S_i^+}\,\overline{S_j^-} + \overline{S_i^-}\,\overline{S_j^+}) - \tfrac{1}{2}\sin^2\phi(\overline{S_i^+}\,\overline{S_j^+} + \overline{S_i^-}\,\overline{S_j^-})] - B_z\cos\phi\sum_i \overline{S_i^z} - B_z\sin\phi\left(\sum_{i\in A}\overline{S_i^x} - \sum_{j\in B}\overline{S_j^x}\right), \tag{A3}$$

with $i \in A$ and $j \in B$. The summation over $\langle ij\rangle$ includes each pair of nearest neighbors only once.

The spin waves for the Hamiltonian (A3) are found by writing the equations of motion for the Green functions,[50]

$$\langle\langle S_i^+ | S_l^-\rangle\rangle = \frac{1}{\pi}\langle S_i^z\rangle\delta_{il} + \langle\langle [S_i^+, H] | S_l^-\rangle\rangle, \tag{A4}$$

and performing the random-phase approximation, which in our case means the decoupling

$$\langle\langle S_i^+ S_j^z | S_l^-\rangle\rangle \simeq \langle S_j^z\rangle\langle\langle S_i^+ | S_l^-\rangle\rangle, \tag{A5}$$

etc. The reference symmetry-broken state for the rotated Hamiltonian (A3) has the spins on both sublattices pointing upwards, and thus we implement in Eq. (A5) the classical averages for all $i$,

$$\langle S_i^z\rangle = S. \tag{A6}$$

The RPA problem is now a $4\times4$ matrix, since the $S_i^+$ and $S_i^-$ operators are coupled. (In the quantum antiferromagnet, equivalent to the present problem at half filling, the RPA problem is $2\times2$.) Taking the sequence of operators: $S_A^+$, $S_B^+$, $S_A^-$, $S_B^-$, one finds in $\vec{k}$ space the eigenvalue problem,

$$\begin{pmatrix} a-\omega & b\gamma_{\vec{k}} & 0 & -c\gamma_{\vec{k}} \\ b\gamma_{\vec{k}} & a-\omega & -c\gamma_{\vec{k}} & 0 \\ 0 & c\gamma_{\vec{k}} & -a-\omega & -b\gamma_{\vec{k}} \\ c\gamma_{\vec{k}} & 0 & -b\gamma_{\vec{k}} & -a-\omega \end{pmatrix} \begin{pmatrix} \langle\langle S_A^+|\cdots\rangle\rangle \\ \langle\langle S_B^+|\cdots\rangle\rangle \\ \langle\langle S_A^-|\cdots\rangle\rangle \\ \langle\langle S_B^-|\cdots\rangle\rangle \end{pmatrix} = 0, \tag{A7}$$

where we made use of Eq. (A1) to eliminate the external field $B_z$ (A1) imposing the constraint, and we have introduced the following definitions:

$$a = JzS,$$
$$b = JzS\cos^2\phi,$$
$$c = JzS\sin^2\phi. \tag{A8}$$

From Eq. (A7) one finds easily the RPA spectrum,

$$\omega_{\vec{k}} = \pm[(a \pm b\gamma_{\vec{k}})^2 - c^2\gamma_{\vec{k}}^2]^{1/2}, \tag{A9}$$

defined in the folded Brillouin zone which corresponds to the two-sublattice magnetic structure. The dispersion relation is linear in $k$ at $\vec{k}\to\vec{0}$, with the stiffness constant decreasing when the spins approach the ferromagnetic order ($\phi\to 0$),

$$\omega_{\vec{k}}\simeq\frac{1}{2}\sqrt{1-\cos(2\phi)}\;k, \tag{A10}$$

and one finds the usual logarithmic term in the quantum correction of the order parameter of a 2D system. The order parameter is related to the local spin-flip correlation function,

$$\langle S_i^z\rangle = S-\langle S_i^- S_i^+\rangle, \tag{A11}$$

calculated from the respective Green function using the fluctuation-dissipation theorem,[50]

$$\langle S_i^- S_i^+\rangle = \int_{\infty}^{-\infty} d\omega\;\frac{2\,\mathrm{Im}\langle\langle S_i^+|S_i^-\rangle\rangle_{\omega-i\epsilon}}{\exp(\beta\omega)-1}, \tag{A12}$$

with $\beta=1/k_BT$. The ground-state energy $E_0$ is found in the standard way[50] by calculating the individual correlation functions which enter in the expansion of the Hamiltonian (A3) up to lowest order, and making use of relations similar to Eq. (A12). This is equivalent to rewriting the effective RPA Hamiltonian in normal order and next summing up the zero-point motion contributions.[51]

Unfortunately, the lowest-order RPA calculation of the individual off-diagonal quantities, $\langle S_i^+ S_j^-\rangle$ and $\langle S_i^z S_j^z\rangle$, Eq. (2.13), does not give satisfactory answers, in spite of rather accurate estimation of both the total energy and the order parameter (A11). For example, starting from a 2D Néel state with the moments in $z$ direction one finds for the nearest neighbors that $\langle S_i^+ S_j^-\rangle_{\mathrm{RPA}}\simeq -0.2756$, and $\langle S_i^z S_j^z\rangle_{\mathrm{RPA}}\simeq -0.0534$, while the assumed LRO in the $z$ direction implies that $|\langle S_i^+ S_j^-\rangle|<2|\langle S_i^z S_j^z\rangle|$.

To obtain more accurate numbers for these intersite spin-spin correlation functions we extend the LSW and include also second-order terms. First, we expand the local magnetization in terms of Holstein-Primakoff bosons $b_i^\dagger$ and $b_i$,[20]

$$S_i^z = S-b_i^\dagger b_i. \tag{A13}$$

The corresponding representation of $S_i^\pm$ operators is

$$S_i^+=\sqrt{2S}\,\sqrt{1-\frac{b_i^\dagger b_i}{2S}}\;b_i,$$

$$S_i^-=\sqrt{2S}\,b_i^+\,\sqrt{1-\frac{b_i^\dagger b_i}{2S}}. \tag{A14}$$

The ground-state energy $E_0$ is given by the longitudinal ($S^{zz}$) and transverse ($S^{+-}$) spin-spin correlation functions,

$$E_0=\cos(2\phi)S^{zz}_{\mathrm{RPA}}+S^{+-}_{\mathrm{RPA}}. \tag{A15}$$

We express the energy $E_0$ in terms of the Holstein-Primakoff bosons using Eq. (A11), and the expansion of the square root in Eqs. (A14) up to lowest order $\sim b_i^\dagger b_i$. As a result one finds that the ground-state energy (A15) per one bond reads

$$E_0=J\cos(2\phi)\langle(S-b_i^\dagger b_i)(S-b_j^\dagger b_j)\rangle + JS\left\langle(b_i^\dagger b_j+b_j^\dagger b_i)\left(1-\frac{1}{4S}b_i^\dagger b_i-\frac{1}{4S}b_j^\dagger b_j\right)\right\rangle. \tag{A16}$$

Keeping only the terms containing up to four boson operators, factorizing the higher-order averages by implementing the Wicks theorem, and making use of the symmetry between the two sublattices, one finds a simplified relation [here $n_b=\langle b_i^\dagger b_i\rangle$ is the reduction of the magnetization, see Eq. (A13)],

$$E_0=J\cos(2\phi)[(S-n_b)^2+\langle b_i^\dagger b_j\rangle^2]+2J(S-n_b)\langle b_i^\dagger b_j\rangle. \tag{A17}$$

Equation (A17) is used to determine the off-diagonal average of the boson operators, $\langle b_i^\dagger b_j\rangle$. Using the values of the energy $E_0$ and of the order parameter $\langle S_i^z\rangle$ found in RPA, one is able to determine the nearest-neighbor spin correlations from the two terms which contribute to Eq. (A17),

$$S^{zz}=\cos(2\phi)[(S-n_b)^2+\langle b_i^\dagger b_j\rangle^2],$$

$$S^{+-}=2(S-n_b)\langle b_i^\dagger b_j\rangle. \tag{A18}$$

The quality of this approximation may be best illustrated on the example of a 2D antiferromagnet, where it gives $\langle S_i^z S_j^z\rangle\simeq -0.1650$, which is a considerably lower value than one-third of the scalar product of spin operators in LSW theory, $\langle\vec{S}_i\vec{S}_j\rangle_{\mathrm{LSW}}\simeq -0.3290$, expected for a rotationally invariant ground state in the pseudospin space. The above result for $S^{zz}$ correlation function agrees very well with the perturbation expansion in local spin-flip processes based on a variational Bartkowski wave function, $\langle S_i^z S_j^z\rangle_{\mathrm{var}}\simeq -0.1628$.[52]

Calculating the correlation functions $S^{zz}$ and $S^{+-}$ from Eqs. (A18) one has to keep in mind that the $z$ axis has been chosen along the magnetization direction. This choice would correspond to the CDW ground state at half filling ($n=1$). On the contrary, the spins lie within the $(x,y)$ plane in the SS phase at half filling, and form an angle $\pm\phi$ with the field $B_z$ at $n<1$. Thus the spin-spin correlation functions $S^{zz}_{\mathrm{SS}}$ and $S^{+-}_{\mathrm{SS}}$ are calculated in the SS phase by projecting the quantities found above Eq. (A18) on the directions parallel and perpendicular to the field direction, respectively,

$$S^{zz}_{\mathrm{SS}}=\cos^2\phi S^{zz}+\frac{1}{2}\sin^2\phi S^{+-},$$

$$S^{+-}_{\mathrm{SS}}=-\sin^2\phi S^{zz}+\frac{1}{2}(1+\cos^2\phi)S^{+-}. \tag{A19}$$

The numerical results for these correlation functions ($S^{zz}_{\mathrm{SS}}$ and $S^{+-}_{\mathrm{SS}}$) away from the limit of quantum antiferromagnet ($n=1$) are shown in Fig. 2(b), and applied in Sec. IV to calculate the weight of the LHB and UHB in optical spectroscopy for 2D and 3D lattices. In the classical ($D\to\infty$) limit the quantum fluctuations vanish, $S^{+-}=0$, and the spin-spin correlations in the ground state are directly obtained from Eqs. (A19) using $S^{zz}=1/4$.

## APPENDIX B: TWO-POLE ANSATZ

The best possible approximation to the $\vec{k}$-dependent one-particle spectral function using only two $\delta$ functions,[28,29]

$$A_{\vec{k}\sigma}(\omega)=\sum_{i=1,2} w_{i,\vec{k}\sigma}\delta(\omega-\varepsilon_{i,\vec{k}\sigma}), \tag{B1}$$

is obtained when the four coefficients are determined by the four lowest moments (zeroth to third) of the spectrum. This two-pole ansatz has been used recently by Micnas *et al.*[34] and by Schneider, Penderson, and Rodríguez-Núñez[35] who showed that it agrees well with the $T$-matrix approximation in the low density limit.

The spectral weights $w_{i,\vec{k}\sigma}$ and the pole energies $\varepsilon_{i,\vec{k}\sigma}$ depend not only on the lattice structure ($\epsilon_{\vec{k}}$) and particle density ($n_\sigma=\langle n_{i\sigma}\rangle$), as in the Hubbard I approach,[53] but also on the two-site correlation functions. These correlations enter via the third moment,

$$m^{(3)}_{\vec{k}\sigma}=U^3 n_{\bar{\sigma}}+U^2[n_{\bar{\sigma}}(n_{\bar{\sigma}}+2)\epsilon_{\vec{k}}+B_{\vec{k}\sigma}]+3Un_{\bar{\sigma}}\epsilon^2_{\vec{k}}+\epsilon^3_{\vec{k}}, \tag{B2}$$

where

$$B_{\vec{k}\sigma}=\frac{t}{N_a}\sum_{i,\delta}[\langle(1-n_{i\sigma})a^\dagger_{i\bar{\sigma}}a_{i+\delta,\bar{\sigma}}(1-n_{i+\delta,\sigma})\rangle - \langle n_{i\sigma}a^\dagger_{i\bar{\sigma}}a_{i+\delta,\bar{\sigma}}n_{i+\delta,\sigma}\rangle]+\epsilon_{\vec{k}}(\langle n_{i\bar{\sigma}}n_{i+\delta,\bar{\sigma}}\rangle-n^2_{\bar{\sigma}} - \langle a^\dagger_{i\sigma}a^\dagger_{i+\delta,\bar{\sigma}}a_{i\bar{\sigma}}a_{i+\delta,\sigma}\rangle-\langle a^\dagger_{i,\sigma}a^\dagger_{i,\bar{\sigma}}a_{i+\delta,\bar{\sigma}}a_{i+\delta,\sigma}\rangle). \tag{B3}$$

If $|U|\gg t$, the two poles will correspond to the LHB and UHB. Their spectral intensities can be identified as $w_{1,\vec{k}\sigma}$ and $w_{2,\vec{k}\sigma}$, respectively. We have shown before, for positive $U$, that an expansion to first order in $t/U$ of the two-pole ansatz is equivalent to the perturbation theory.[19,54] Expanding Eq. (B1) for large negative $U$, one finds the weights $w_{1,\vec{k}\sigma}=1-n/2$ and $w_{2,\vec{k}\sigma}=n/2$. Thus the weights found in Sec. III B are reproduced.

As the ground state consists only of local pairs and empty sites in the large-negative-$U$ limit, all kinetic expectation values are zero and the $\vec{k}$-independent part of $B_{\vec{k}\sigma}$ vanishes. The $\vec{k}$-dependent part of $B_{\vec{k}\sigma}$, however, *is crucial and cannot be replaced by its average over the Brillouin zone* ($=0$). In fact, the $\vec{k}$-dependent term contains in this case information about nearest-neighbor correlation functions which makes the two-pole ansatz more realistic than the Hubbard I approximation. By expanding the pole energies given by Eqs. (77) of Ref. 19 in the large-attractive-$U$ limit one recovers the momentum-dependent energies Eqs. (3.18) and (3.19). If the momentum-dependent term in $B_{\vec{k}\sigma}$ is neglected, as is often done in a self-consistent two-pole treatment, incorrect and qualitatively different results are obtained.[35] By expanding the pole energies given by Eqs. (77) of Ref. 18 in the large-$|U|$ limit one finds

$$\varepsilon_{1,\vec{k}\sigma}=\epsilon_{\vec{k}}\left[1+\frac{2}{2-n}\left(\langle\vec{S}_i\cdot\vec{S}_{i+\delta}\rangle-\frac{1}{4}\right)\right],$$

$$\varepsilon_{2,\vec{k}\sigma}=-|U|+\epsilon_{\vec{k}}\left[1+\frac{2}{n}\left(\langle\vec{S}_i\cdot\vec{S}_{i+\delta}\rangle-\frac{1}{4}\right)\right]. \tag{B4}$$

Thus we recover Eqs. (3.18) and (3.19) derived in Sec. III B. for the UHB and LHB, respectively, with $\langle\vec{S}_i\cdot\vec{S}_{i+\delta}\rangle$ being the pseudospin correlation function which follows from the mapping of Sec. II.

In the classical ($D\to\infty$) limit one has $\langle\vec{S}_i\cdot\vec{S}_{i+\delta}\rangle=-n(1-n/2)+1/4$, and thus

$$\varepsilon_{1,\vec{k}\sigma}=(1-n)\epsilon_{\vec{k}},$$

$$\varepsilon_{2,\vec{k}\sigma}=-|U|+(n-1)\epsilon_{\vec{k}}. \tag{B5}$$

This is plotted in Fig. 5. The $\vec{k}$ dependence vanishes at $n=1$ as the motion of a single electron or hole in $U<0$ case becomes then equivalent to the result of Brinkman and Rice for the motion of a hole doped to classical antiferromagnet.[36]

*Permanent address: Institute of Physics, Jagellonian University, Reymonta 4, PL-30 059 Kraków, Poland.


[1] R. Micnas, J. Ranninger, and S. Robaszkiewicz, Rev. Mod. Phys. **62**, 113 (1990) and references therein; S. Robaszkiewicz, R. Micnas, and K.A. Chao, Phys. Rev. B **23**, 1447 (1981).

[2] C. M. Varma, Phys. Rev. Lett. **61**, 2713 (1988).

[3] A. Taraphder, H. K. Krishnamurthy, R. Pandit, and T. V. Ramakrishnan, Phys. Rev. B **52**, 1368 (1995).

[4] One should be careful, however, when comparing the experiments with a purely electronic model, since lattice distortions due to the strong electron-phonon coupling will have very similar effects and also stabilize the CDW state.

[5] P. Pincus, P. Chaikin, and C. F. Coll III, Solid State Commun. **12**, 1265 (1973).

[6] J. O. Sofo, C. A. Balseiro, and H. E. Castillo, Phys. Rev. B **45**, 9860 (1992).

[7] P. Nozières and S. Schmitt-Rink, J. Low Temp. Phys. **59**, 195 (1985).

[8] P. J. H. Denteneer, G. An, and J. M. J. van Leeuwen, Europhys. Lett. **16**, 5 (1991).

[9] Y. Ohta, A. Nakauchi, R. Eder, K. Tsutsui, and S. Maekawa, Phys. Rev. B **52**, 15 617 (1995).

[10] S. L. Cooper *et al.*, Phys. Rev. B **41**, 11 605 (1990); **45**, 2549 (1992); S. Uchida, T. Ido, H. Takagi, T. Arima, Y. Tokura, and S. Tajima, *ibid.* **43**, 7942 (1991).

[11] H. Romberg, M. Alexander, N. Nücker, P. Adelmann, and J. Fink, Phys. Rev. B **42**, 8768 (1990); C. T. Chen *et al.*, Phys. Rev. Lett. **66**, 104 (1991).

[12] T. Katsufuji, Y. Okimoto, and Y. Tokura, Phys. Rev. Lett. **75**, 3497 (1995).

[13] M. S. Hybertsen, E. B. Stechel, W. M. C. Foulkes, and M. Schlüter, Phys. Rev. B **45**, 10 032 (1992).

[14] H. Eskes, M. B. J. Meinders, and G. A. Sawatzky, Phys. Rev. Lett. **67**, 1035 (1991); M. B. J. Meinders, H. Eskes, and G. A. Sawatzky, Phys. Rev. B **48**, 3916 (1993).

[15] A. M. Oleś, G. Tréglia, D. Spanjaard, and R. Jullien, Phys. Rev. B **34**, 5101 (1986).

[16] Y. Ohta, K. Tsutsui, W. Koshibae, T. Shmozato, and S. Maekawa, Phys. Rev. B **46**, 14 022 (1992).

[17] A. B. Harris and R. V. Lange, Phys. Rev. **157**, 295 (1967).
[18] H. Eskes and A. M. Oleś, Phys. Rev. Lett. **73**, 1279 (1994).
[19] H. Eskes, A. M. Oleś, M. B. J. Meinders, and W. Stephan, Phys. Rev. B **50**, 17 980 (1994).
[20] A. Auerbach, *Interacting Electrons and Quantum Magnetism* (Springer, New York, 1994).
[21] E. H. Lieb, Phys. Rev. Lett. **62**, 1201 (1989).
[22] H. Shiba, Prog. Theor. Phys. **48**, 2171 (1972).
[23] Y. Nagaoka, Prog. Theor. Phys. **52**, 1716 (1974).
[24] C. N. Yang, Phys. Rev. Lett. **63**, 2144 (1989).
[25] See, for instance, A. Montorsi and D. K. Campbell, Phys. Rev. B **53**, 5133 (1996), and the references therein.
[26] A. G. Rojo, J. O. Sofo, and C. A. Balseiro, Phys. Rev. B **42**, 10 241 (1990).
[27] K. A. Chao, J. Spałek, and A. M. Oleś, J. Phys. C **10**, L271 (1977); Phys. Rev. B **18**, 3453 (1978).
[28] L. Roth, Phys. Rev. **184**, 451 (1969).
[29] G. Geipel and W. Nolting, Phys. Rev. B **38**, 2608 (1988).
[30] A. Moreo, D. J. Scalapino, and S. R. White, Phys. Rev. B **45**, 7544 (1992).
[31] E. Dagotto, A. Moreo, F. Ortolani, J. Riera, and D. J. Scalapino, Phys. Rev. Lett. **67**, 1918 (1991).
[32] H. E. Castillo and C. A. Balseiro, Phys. Rev. B **45**, 10 549 (1992).
[33] S. V. Traven, J. Phys. Condens. Matter **6**, 5839 (1994).
[34] R. Micnas, M. H. Pedersen, S. Schafroth, T. Schneider, J. J. Rodríguez-Núñez, and H. Beck, Phys. Rev. B **52**, 16 233 (1995).
[35] T. Schneider, M. H. Penderson, and J. J. Rodríguez-Núñez, Z. Phys. B **100**, 263 (1996).
[36] W. F. Brinkman and T. M. Rice, Phys. Rev. B **2**, 1324 (1970).
[37] L. N. Bulaevskiĭ and D. I. Khomskiĭ, Zh. Éksp. Teor. Fiz. **52**, 1603 (1967) [Sov. Phys. JETP **25**, 1067 (1967)].
[38] R. B. Griffiths, Phys. Rev. **133**, A768 (1964).
[39] N. Kawakami and S.-K. Yang, Phys. Rev. B **44**, 7844 (1991).
[40] E. Dagotto, A. Moreo, F. Ortolani, J. Riera, and D. J. Scalapino, Phys. Rev. B **45**, 10 107 (1992).
[41] R. M. Fye, M. J. Martins, D. J. Scalapino, J. Wagner, and W. Hanke, Phys. Rev. B **45**, 7311 (1992).
[42] G. D. Mahan, *Many Particle Physics* (Plenum Press, New York, 1981), Chap. 1.
[43] W. Kohn, Phys. Rev. **133**, A171 (1964).
[44] P. F. Maldague, Phys. Rev. B **16**, 2437 (1977).
[45] B. S. Shastry and B. Sutherland, Phys. Rev. Lett. **65**, 243 (1990).
[46] A. Georges, G. Kotliar, W. Krauth, and M. J. Rozenberg, Rev. Mod. Phys. **68**, 13 (1996).
[47] T. B. Bahder and F. Woynarovich, Phys. Rev. B **33**, 2114 (1986).
[48] M. A. Karlow, S. L. Cooper, A. L. Kotz, M. V. Klein, P. D. Han, and D. A. Payne, Phys. Rev. B **48**, 6499 (1993).
[49] U. Hahn, G. Vielsack, and W. Weber, Phys. Rev. B **49**, 15 936 (1994).
[50] D. N. Zubarev, Usp. Fiz. Nauk. **71**, 71 (1960) [Sov. Phys. Usp. **3**, 320 (1960)]; S. B. Haley and P. Erdös, Phys. Rev. B **5**, 1106 (1972).
[51] L. F. Feiner, A. M. Oleś, and J. Zaanen (unpublished).
[52] A. M. Oleś and B. Oleś, J. Phys. Condens. Matter **5**, 8403 (1993).
[53] J. Hubbard, Proc. R. Soc. London, Ser. A **276**, 238 (1963).
[54] A. M. Oleś and H. Eskes, Physica B **206-207**, 685 (1995).